PHYSICAL REVIEW C VOLUME 3, NUMBER 6 JUNE 1971

Effect of the Multipole Pairing and Particle-Hole Fields in the Particle-Vibration Coupling of ^{209}Pb. I.*

D. R. Bes and R. A. Broglia†
Los Alamos Scientific Laboratory, University of California, Los Alamos, New Mexico 87544, and School of Physics and Astronomy, University of Minnesota, Minneapolis, Minnesota 55455

(Received 12 October 1970)

The particle-vibration-coupling formalism for nuclei around closed shells is studied and a microscopic description is given. We consider as collective modes of excitation of the closed-shell-system (N_0) ground state both particle-hole excitations and excitations that change the number of particles by 2 (pairing mode). To describe the pairing modes, multipole pairing residual interactions are used. The odd particle is allowed to couple to both types of vibrations. The coupling Hamiltonian is linear in the collective phonons and the particle variables. The effective Hamiltonian is constructed by a perturbative method. Explicit expressions are given for the spectroscopic amplitudes and spectroscopic factors associated with the $(N_0-1)(t,p)(N_0+1)$ and $(N_0+2)(p,d)(N_0+1)$ reactions, respectively. The concept of an effective transfer operator is used. Special attention is paid to the ^{207}Pb(t,p) and ^{210}Pb-(p,d) reactions.

I. INTRODUCTION

The lower-energy states of many-body systems may be described in terms of a vacuum state and elementary (independent) excitations. In nuclei, the BCS ground state and the normal ground state constructed with a determinant wave function are the most common vacuum states.

It is convenient to characterize the elementary excitations[1] by their quantum numbers [angular momentum (λ), parity (π), isospin (τ), spin (σ), and transfer (α) quantum numbers]. There is a large amount of literature which is devoted to the study of each type of excitation separately.

The next logical step in difficulty is to consider states which are made up from two elementary excitations. If one of the excitations has a collective character (from the point of view of the extreme shell model) while the second has a single-particle nature, it is customary to construct an interaction Hamiltonian which is linear in the collective and particle variables. For instance, in deformed nuclei, states of the odd system are formed by a quasiparticle excitation ($|\alpha| = 1$) and a rotational excitation ($\alpha = 0$). The corresponding Coriolis coupling is proportional to the frequency of the rotational motion and to the single-particle angular momentum.[2]

The coupling between the quasiparticles and vibrations (both in spherical[3] and in deformed nuclei[4]), or the coupling between particles (holes) and vibrations of the normal systems, has not yielded a picture as accurate as in the case of rotations. Moreover, until recently the available experimental data have been able to check the properties of only lower predicted states.

In 1967, rather complete experimental information on the members of the multiplet of states built by coupling the low-lying octupole phonon ($\lambda = 3$, $\alpha = 0$) of ^{208}Pb with single-particle proton states became available.[5] Mottelson[6] suggested that a systematic application of perturbation theory should be required in order to understand the coupling. Since then, this approach has been applied in a number of papers.[7]

Similar information as the one obtained in ^{209}Bi quoted previously is reported in the following paper of this issue.[8] The underlying theory of the theoretical predictions reported there is developed in the following sections. The basis of this theoretical approach is found in Ref. 6. To account for the experimental data, we have included in our description both the $\alpha = 2$ and $\alpha = 0$ elementary modes of excitation of ^{208}Pb.

II. COLLECTIVE DEGREES OF FREEDOM

In this section, some of the collective degrees of freedom of the normal system are discussed, and the corresponding solutions are presented.

A. Multipole Pairing Fields

The existence of enhanced two-nucleon transitions with $J^\pi = 0^+, 2^+, 4^+, \ldots$ to the $N_0 \pm 2$ system, starting from the closed-shell (N_0) ground state, suggests the existence of multipole pairing fields of multipolarity $\lambda = 0, 2, 4, \ldots$. In addition to the multipolarity λ, the field is characterized by the isospin $\tau = 1$, the spin $\sigma = 0$, and the transfer quantum number $\alpha = \pm 2$.[1,9]

These fields may be produced by a separable pairing interaction that scatters pairs of particles coupled to λ. The corresponding matrix elements of the interaction can be defined in complete anal-

ogy with what is done in the monopole ($\lambda = 0$) pairing case.[10] One ensures that the matrix elements of the pairing force, in the angular momentum channel considered, have the same phase as the matrix elements of a δ force (see Appendix I). Particles interacting through this force have a high degree of spatial correlation in the lowest state of each spin λ and parity $(-1)^\lambda$. These particles spend a fraction of their time in a relative s state, while the center of mass carries an angular momentum λ. This fraction, though in principle small, is much larger than that spent by uncorrelated particles. All the contributions to the cross section of a two-particle transfer reaction leading to this correlated state add up coherently. The pairing interaction is written

$$H(2\lambda) = -G_\lambda \pi (2\lambda+1) \sum_\mu P_{\lambda\mu}^\dagger P_{\lambda\mu}, \tag{1}$$

where

$$P_{\lambda\mu}^\dagger = -\frac{2}{(2\lambda+1)^{1/2}} \Big[\sum_{k_1 \geq k_2} \frac{M(k_1k_2;\lambda)}{(1+\delta_{12})^{1/2}} \beta^\dagger(k_1k_2;2\lambda\mu) + \sum_{i_1 \geq i_2} \frac{M(i_1i_2;\lambda)}{(1+\delta_{12})^{1/2}} (-1)^{\lambda-\mu} \beta(i_1i_2;-2\lambda-\mu) \Big], \tag{2a}$$

$$\beta^\dagger(i_1i_2;-2\lambda\mu) = \frac{1}{(1+\delta_{12})^{1/2}} [b_{i_1} b_{i_2}]_\mu^\lambda, \tag{2b}$$

$$\beta^\dagger(k_1k_2;2\lambda\mu) = \frac{1}{(1+\delta_{12})^{1/2}} [b_{k_1}^\dagger b_{k_2}^\dagger]_\mu^\lambda. \tag{2c}$$

Here $b_j^\dagger$ creates a particle in an orbital j. The label k denotes states above the Fermi surface while i denotes states below the Fermi surface. The index j is used to denote either states k or i. The particle creation operators $b_j^\dagger$ transform under time reversal as

$$\tau b_{jm}^\dagger \tau^{-1} = (-1)^{j-m} b_{j-m}^\dagger. \tag{2d}$$

The coefficients $M(j_1j_2;\lambda)$ are defined as

$$M(j_1j_2;\lambda) = \langle j_1 \| f_\lambda(r) Y_\lambda \| j_2 \rangle i^{l_{j_2}-l_{j_1}+\lambda} = M(j_2j_1;\lambda)(-1)^{j_1-j_2+\lambda}. \tag{2e}$$

The detailed radial dependence of $f_\lambda(r)$ is irrelevant to a large extent, provided it is peaked around the nuclear surface. The reduced matrix elements $\langle j_1 \| Y_\lambda \| j_2 \rangle$ are calculated assuming the usual Condon-Shortley convention. The pair addition and removal collective phonons are defined as

$$\beta_n^\dagger(2\lambda\mu) = \sum_{k_1 \geq k_2} d_n(k_1k_2;2\lambda) \beta^\dagger(k_1k_2;2\lambda\mu) - (-1)^{\lambda-\mu} \sum_{i_1 \geq i_2} d_n(i_1i_2;2\lambda) \beta(i_1i_2;2\lambda-\mu), \tag{3a}$$

$$\beta_n^\dagger(-2\lambda\mu) = \sum_{i_1 \geq i_2} d_n(i_1i_2;-2\lambda) \beta^\dagger(i_1i_2;-2\lambda\mu) - (-1)^{\lambda-\mu} \sum_{k_1 \geq k_2} d_n(k_1k_2;-2\lambda) \beta(k_1k_2;-2\lambda-\mu). \tag{3b}$$

These are the quanta associated with the two collective modes of the Hamiltonian in Eq. (1) for normal systems, that is, systems where $G_\lambda < G_\lambda^c$ (G_λ^c being the smallest value of the multipole pairing coupling constant for which the BCS number and gap equations have a solution). The pairing modes have transfer number $\alpha = \pm 2$ and correspond to states of the $N_0 \pm 2$ nucleus, where N_0 stands for a magic number of either protons or neutrons.

Diagonalizing the Hamiltonian $H_{sp} + H(2\lambda)$ in the linearization approximation [random-phase approximation (RPA)] gives

$$\frac{1}{4\pi G_\lambda} = \sum_{k_1,k_2} \frac{|M(k_1k_2;\lambda)|^2}{E_{k_1k_2} \mp W_n(\pm 2\lambda)} + \sum_{i_1,i_2} \frac{|M(i_1i_2;\lambda)|^2}{E_{i_1i_2} \pm W_n(\pm 2\lambda)}, \tag{4}$$

where $H_{sp} = \sum_j \epsilon_j b_j^\dagger b_j$ is the single-particle Hamiltonian, $E_{j_1j_2} = \epsilon_{j_1} + \epsilon_{j_2}$ the energy of a two-particle (two-hole) state, and $W_n(\alpha\lambda)$ the energy of the nth collective mode of excitation, with angular momentum λ, of the system with $N_0 + \alpha$ particles. The corresponding amplitudes defining the phonons (3a) and (3b) are

$$\begin{aligned} d_n(k_1k_2;2\lambda) &= \frac{\Lambda_n(2\lambda)}{(1+\delta_{12})^{1/2}} \frac{M(k_1k_2;\lambda)}{E_{k_1k_2} - W_n(2\lambda)}, \\ d_n(i_1i_2;2\lambda) &= \frac{\Lambda_n(2\lambda)}{(1+\delta_{12})^{1/2}} \frac{M(i_1i_2;\lambda)}{E_{i_1i_2} + W_n(2\lambda)}, \\ d_n(i_1i_2;-2\lambda) &= \frac{\Lambda_n(-2\lambda)}{(1+\delta_{12})^{1/2}} \frac{M(i_1i_2;\lambda)}{E_{i_1i_2} - W_n(-2\lambda)}, \\ d_n(k_1k_2;-2\lambda) &= \frac{\Lambda_n(-2\lambda)}{(1+\delta_{12})^{1/2}} \frac{M(k_1k_2;\lambda)}{E_{k_1k_2} + W_n(-2\lambda)}, \end{aligned} \tag{5}$$

where

$$\Lambda_n(\pm 2\lambda) = \sqrt{2} \Big\{ \pm \sum_{k_1,k_2} \frac{|M(k_1k_2;\lambda)|^2}{[E_{k_1k_2} \mp W_n(\pm 2\lambda)]^2} \mp \sum_{i_1,i_2} \frac{|M(i_1i_2;\lambda)|^2}{[E_{i_1i_2} \pm W_n(\pm 2\lambda)]^2} \Big\}^{-1/2}. \tag{6}$$

The magnitudes given in Eq. (6) are obtained from the usual normalization conditions

$$\sum_{k_1 \geq k_2} [d_n(k_1k_2;\pm 2\lambda)]^2 - \sum_{i_1 \geq i_2} [d_n(i_1i_2;\pm 2\lambda)]^2 = \pm 1. \tag{7}$$

The multipole pairing coupling constants G_λ may be fixed either by using the energy of the lowest

$J=\lambda$, $\pi=(-1)^\lambda$ state of the $N_0\pm 2$ systems in Eq. (4), or by fitting the two-particle transfer cross section to the lowest state of each spin and parity. The spectroscopic amplitudes[11] $B(j_1 j_2; n\alpha J)$ are equal to

$$B(j_1 j_2{:}n2J) \equiv \frac{\langle 1(n2\lambda); JM|[b_{j_1}^\dagger b_{j_2}^\dagger]_M^J|0\rangle}{(1+\delta_{j_1 j_2})^{1/2}} = d_n(j_1 j_2; 2\lambda)\,,$$

$$B(j_1 j_2; n-2J) \tag{8}$$

$$\equiv \frac{\langle 1(n-2\lambda); JM|[b_{j_1} b_{j_2}]_M^J|0\rangle}{(1+\delta_{j_1 j_2})^{1/2}} = d_n(j_1 j_2; -2\lambda)\,,$$

where $|\nu(n\pm 2\lambda); JM\rangle$ ($\nu=1$) is a one-phonon state of the $N_0+\alpha$ system generated by the operator $\beta_n^\dagger(\pm 2\lambda\mu)$ (of course, $\lambda=J$) acting on the N_0 ground state $|0\rangle$ (see end of this section and Sec. 4A). The (t,p) and (p,t) cross sections are then proportional to $\Lambda_n^2(2\lambda)$ and $\Lambda_n^2(-2\lambda)$, respectively.

The usual distorted-wave calculation of two-body transfer processes yields reliable relative cross sections but fails to reproduce absolute cross sections. Therefore, we may write

$$\sigma_{\rm exp}(N_0, J, \alpha) = R\sigma_{\rm th}(N_0, J, \alpha)\,, \tag{8'}$$

where the normalization factor $R=\sigma_{\rm exp}/\sigma_{\rm th}$ can be better determined for the case of ground state ($J=0$) transition.[12] This is so because the parameter G_0 [and consequently $\Lambda_1(2\dot{0})$ and $\Lambda_1(-20)$], which corresponds to the usual monopole case, is rather well known from the systematic data available on the odd-even mass difference. Once the normalization factor is known, the parameters $\Lambda_n(2\lambda)$ and $\Lambda_n(-2\lambda)$ for $\lambda\neq 0$ can be determined, and consequently G_λ through Eq. (8'). In the present paper the levels ^{206}Pb(J^π) and ^{210}Pb(J^π) with $J^\pi=0^+$, 2^+, 4^+, 6^+, and 8^+ are described as pair subtraction and addition modes[13] of ^{208}Pb (g.s.). The corresponding coupling constants, eigenvalues, and Λ factors are displayed in Table I. They are obtained using information concerning only the energy of the levels, and not cross sections. In Fig. 1, we illustrate the method of calculation for $\lambda^\pi=0^+$ and 2^+.

The structure of the pair addition phonon is checked by analyzing the ^{208}Pb(t,p) reaction. The relative cross sections, normalized with respect to the ground-state cross section are displayed in Table II together with the experimental numbers. Through these magnitudes we test the specific

TABLE I. Parameters defining the structure of the pairing and particle-hole collective modes. The magnitude $\Delta W_1(\alpha\lambda)$ [see Eq. (29)] measures the distance between the lowest unperturbed configuration with transfer number α that can couple to total angular momentum λ and parity $(-1)^\lambda$ and the experimental energy (E. Flynn, G. Igo, P. Barnes, and K. Ellegaard, to be published) of the lowest state with these quantum numbers. The quantities $\Delta W_1(\alpha\lambda)$ determine completely the corresponding RPA solution through Eqs. (4), (6), (13), and (15), and consequently all the other magnitudes displayed in the present table; they were taken directly from the experimental spectrum of the even nuclei with the exception of the 6^+ and 8^+ cases (see text). The coupling constants

$$\begin{Bmatrix} G_\lambda \\ \chi_\lambda \end{Bmatrix} = \begin{Bmatrix} g_\lambda \\ k_\lambda \end{Bmatrix} A^{(\lambda/3+1)}[(Mw/\hbar)^\lambda \text{ (MeV)}]\,.$$

The energies $W_1(\alpha\lambda)$ obviously agree with the experimental value because of the choice made for $\Delta W_1(\alpha\lambda)$. The energies $W_n(\alpha\lambda)$ are referred to the ground state of the corresponding even nucleus. The dimensionless parameter $t(\alpha\lambda)$ defined in Eq. (23) measures the strength of the coupling. For $t(\alpha\lambda)\approx 1$, the perturbative treatment of $h(\alpha\lambda)$ breaks down.

		0^+	2^+	4^+	6^+	8^+
^{210}Pb	$g(2\lambda)$ [$(Mw/\hbar)^\lambda$ MeV]	21.38	4.11	0.90	0.21	0.03
	$\Delta W_1(2\lambda)$ (MeV)	1.24	0.44	0.15	0.13	0.10
	$\Lambda_1(2\lambda)$ [$(Mw/\hbar)^{\lambda/2}$ MeV]	1.98	0.86×10^{-1}	0.42×10^{-2}	0.34×10^{-3}	0.20×10^{-4}
	$W_1(2\lambda)$ (MeV)	0.00	0.80	1.09	1.11	1.13
^{206}Pb	$g(-2\lambda)$ (MeV)	21.74	4.03	0.87	0.26	
	$\Delta W_1(-2\lambda)$ (MeV)	0.64	0.41	0.10	0.31	0.31
	$\Lambda_1(-2\lambda)$ [$(Mw/\hbar)^{\lambda/2}$ MeV]	1.73	0.82×10^{-1}	0.34×10^{-2}	0.35×10^{-3}	0.11×10^{-4}
	$W_1(-2\lambda)$ (MeV)	0.00	0.80	1.68	3.25	3.92
	h_λ	0.37	0.22	0.12	0.13	0.12
		2^+	3^-	5^-		
^{208}Pb	$(2\lambda+1)k_\lambda$[$(Mw/\hbar)^\lambda$ MeV]	454.91	113.43	34.3		
	$\Delta W_1(0\lambda)$ (MeV)	0.98	1.36	0.21		
	$\Lambda_1(0\lambda)$[$(Mw/\hbar)^{\lambda/2}$ MeV]	0.15	0.41×10^{-1}	0.10×10^{-3}		
	$W_1(0\lambda)$ (MeV)	4.07	2.62	3.2		
	h_λ	0.28	0.45	0.13		

correlation aspects of the pairing multipole forces. The phonon spectrum is built by the operators $\beta_n^\dagger(\pm 2\lambda\mu)$ and is labeled by the quantum numbers $\nu_1(n_1\alpha_1\lambda_1)I_1$, $\nu_2(n_2\alpha_2\lambda_2)I_2, \ldots; J^\pi$, where ν_i stands for the number of phonons and I_i for the angular momentum to which the phonons of type i are coupled. For $\nu_i = 1$ this quantum number is not required. On the other hand, it may be necessary to specify intermediate-coupling angular momentum to label the state completely. The new degree of freedom added to the pairing field opens a new perspective. For example,[9, 14] it is possible to interpret the $J^\pi = 2^+$ levels excited both in the (t, p) and (p, t) reactions leading to the ^{208}Pb nucleus as states whose main components are

$$|1(1\,2\,2),\ 1(1\,-2\,0);\ 2^+\rangle \equiv |^{210}\mathrm{Pb}(2^+),\ ^{206}\mathrm{Pb}(0^+)\rangle$$

and

$$|1(1\,2\,0),\ 1(1\,-2\,2);\ 2^+\rangle \equiv |^{210}\mathrm{Pb}(0^+),\ ^{206}\mathrm{Pb}(2^+)\rangle.$$

B. Multipole Particle-Hole Fields

In closed-shell nuclei, the low-lying states with angular momentum $J^\pi = 3^-, 5^-, 2^+$ have been successfully described as particle-hole excitations[15] with multipolarity $\lambda = J$, parity $\pi = (-1)^\lambda$, isospin $\tau = 0$, spin $\sigma = 0$, and transfer quantum number $\alpha = 0$. These states have enhanced $B(E\lambda)$ transition probabilities [for example, $B(E3;\ ^{208}\mathrm{Pb},\ \mathrm{g.s.} - 3^-) = 32 B_{sp}$]. The schematic model of such excitations use as residual force a separable multipole-multipole interaction. The corresponding Hamiltonian reads

$$H(0\lambda) = -\frac{\chi_\lambda}{2}\sum_\mu Q_{\lambda\mu} Q_{\lambda\mu}^\dagger, \tag{9}$$

$$Q_{\lambda\mu} = -\frac{1}{(2\lambda+1)^{1/2}}\sum_{k,i} M(ki;\lambda)[\beta^\dagger(ki;0\lambda\mu) + (-1)^{\lambda-\mu}\beta(ki;0\lambda-\mu)], \tag{10}$$

$$\beta^\dagger(ki;0\lambda\mu) = [b_k^\dagger b_i]_\mu^\lambda = \sum_{m_k, m_i}\langle k i m_k m_i | \lambda\mu\rangle \times b_{k m_k}^\dagger (-1)^{i-m_i} b_{i-m_i}, \tag{11a}$$

$$\beta^\dagger(ki;0\lambda\mu) = (-1)^{i-k-\mu}[b_i^\dagger b_k]_{-\mu}^\lambda. \tag{11b}$$

The creation operator of a collective particle-hole

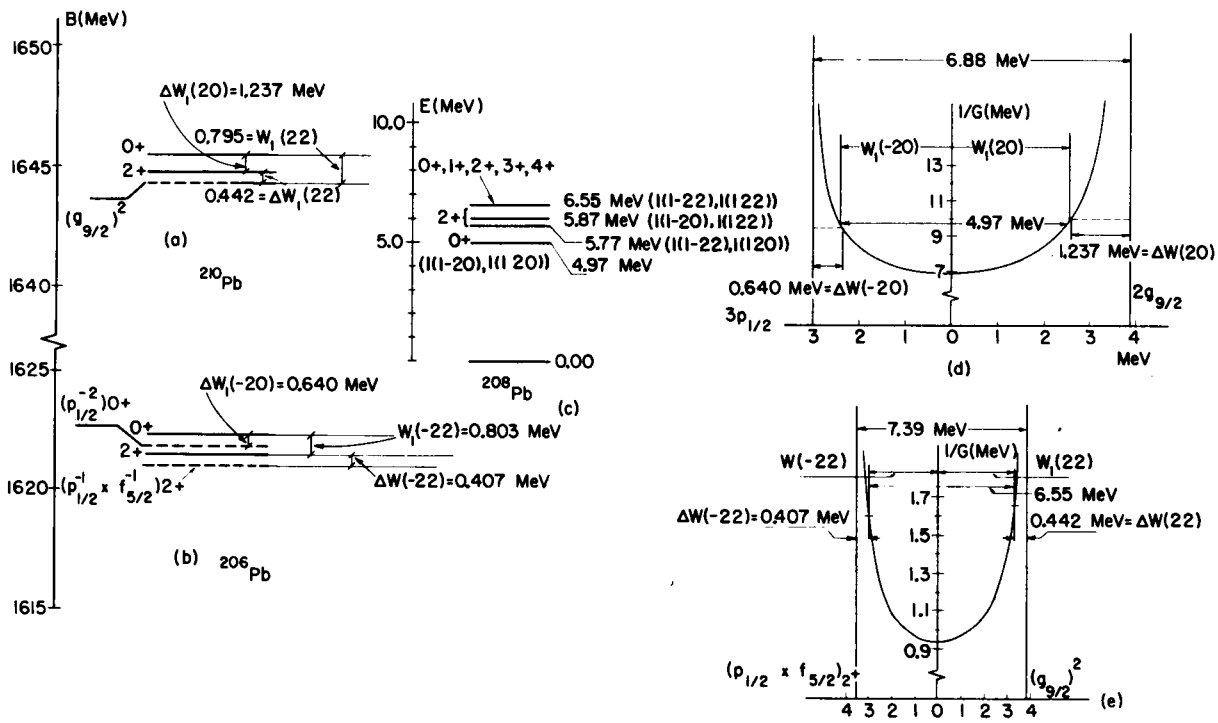

FIG. 1. In (d) and (e) is displayed the left-hand side of the dispersion relations (4) for the case of ^{208}Pb and $\lambda^\pi = 0^+$ (2^+) in the region between the pure two-partial configurations $(p_{1/2}^{-2})$ and $(g_{9/2}^2)$ $[(p_{1/2}^{-1}, f_{5/2}^{-1})$ and $(g_{9/2}^2)]$. For a fixed value of G we can distinguish three sections; (i) The section of the curve at the left gives the gain in energy due to the multipole pairing residual interaction in the nucleus with 206 particles in the 0^+ (2^+) state. (ii) The middle section gives the energy of the two-phonon state in the ^{208}Pb nucleus. The segment to the right gives the gain in binding energy due to the residual multipole pairing force in the nucleus with 210 particles in the lowest 0^+ (2^+) state. In (a) and (b) the above mentioned gain in energy of the ^{206}Pb and ^{210}Pb systems is displayed in terms of the experimental data [J. H. E. Mattauch, W. Thiele, and A. H. Wapstra, Nucl. Phys. 67, 1 (1965)], namely absolute binding energies. In (c), the two-phonon pairing excitations in ^{208}Pb are displayed.

excitation is defined as

$$\beta_n^\dagger(0\lambda\mu) = \sum_{k,i} d_n(ki;0\lambda)\beta^\dagger(ki;0\lambda\mu) - (-1)^{\lambda-\mu}\sum_{k,i} d_n(ik;0\lambda)\beta(ki;0\lambda-\mu)\,. \tag{12}$$

The RPA diagonalization of $H_{sp}+H(0,\lambda)$ gives

$$\frac{1}{\chi_\lambda} = \frac{1}{2\lambda+1}\sum_{k,i}|M(ki;\lambda)|^2\left[\frac{1}{E_{ki}-W_n(0\lambda)}+\frac{1}{E_{ki}+W_n(0\lambda)}\right]. \tag{13}$$

With $E_{ki}=\epsilon_k-\epsilon_i$, the forward- and backward-going amplitudes are given by

$$d_n(ki;0\lambda) = \Lambda_n(0\lambda)\frac{M(ki;\lambda)}{E_{ki}-W_n(0\lambda)}\,, \tag{14a}$$

$$d_n(ik;0\lambda) = \Lambda_n(0\lambda)\frac{M(ki;\lambda)}{E_{ki}+W_n(0\lambda)}\,, \tag{14b}$$

$$\Lambda_n(0\lambda) = \left[\sum_{k,i}|M(ki;\lambda)|^2\left(\frac{1}{[E_{ki}-W_n(0\lambda)]^2} - \frac{1}{[E_{ki}+W_n(0\lambda)]^2}\right)\right]^{-1/2}. \tag{15}$$

TABLE II. Ratio of the theoretical and experimental cross sections (P. Barnes, G. Igo, E. Flynn, and K. Ellegaard, to be published) associated with the low-lying positive-parity states of ^{210}Pb excited in the ^{208}Pb-(t,p) reaction. The normalization factor 310 has been used (Ref. 8). The cross sections defined as $\sum_\theta d\sigma(\theta)/d\Omega$ where $10°\leq\theta\leq 70°$ in steps of 7.5°, were calculated in the distorted-wave Born approximation using as spectroscopic amplitudes the magnitudes defined in Eq. (8). The coefficients $d_n(j_1j_2;\pm 2\lambda)$ were computed for the values of $W_1(2\lambda)$ and $\Lambda_1(2\lambda)$ listed in Table I. Two sets of optical parameters [E. R. Flynn, A. G. Blair, and D. D. Armstrong, Phys. Rev. 170, 1142 (1968)] were used for the triton channel, namely:

(I) $V=148.7$ MeV, $r=1.24$ fm, $a=0.697$ fm,
$W=16.77$ MeV, $r'=1.339$ fm, $a'=0.917$ fm;
(II) $V=167.0$ MeV, $r=1.16$ fm, $a=0.752$ fm,
$W=10.3$ MeV, $r'=1.498$ fm, $a'=0.817$ fm.

In both cases, W stands for the volume absorptive potential depth. Perey's parameters [F. Perey, Phys. Rev. 131, 745 (1965)] were used in the proton channel.

J^π	$\frac{\sigma(^{208}\mathrm{Pb}(t,p)^{210}\mathrm{Pb}(J^\pi))_{th}}{\sigma(^{208}\mathrm{Pb}(t,p)^{210}\mathrm{Pb}(J^\pi))_{exp}}$ I	II
0^+	1.0	1.6
2^+	1.3	1.7
4^+	1.4	1.6
6^+	1.2	1.5
8^+	0.8	1.0

In the same way as in Sec. 2A, it can be shown that the two-body transfer cross section to the one-phonon states generated by the one-phonon operators defined in Eq. (12) is proportional to $[\Lambda_n(0,\lambda)]^2$. In particular, this relation for the lowest state of each spin and parity would determine $W_1(0\lambda)$ through Eq. (15) and consequently χ_λ through Eq. (13).

On the other hand two-nucleon transfer reactions are not specific to excite the surface particle-hole vibrations, but Coulomb excitation or inelastic scattering reactions. The nuclear matrix elements associated with these processes[16] are

$$\langle 1(n0\lambda);JM|[b_k^\dagger b_i]^J_M|0\rangle = d_n(ki;0\lambda)\,,$$
$$\langle 1(n0\lambda);JM|(-1)^{J-M}[b_k^\dagger b_i]^J_{-M}|0\rangle = d_n(ik;0\lambda)\,. \tag{16}$$

In principle then, states with large values of $\Lambda_n(0\lambda)$ would display both large (t,p) cross section and reduced transition probabilities $B(E\lambda)$ (and inelastic scattering cross sections). There is experimental evidence supporting this prediction which has been discussed elsewhere.[17]

The above mentioned correlation is, however, affected by the ground-state correlations. The backward-going amplitudes contribute coherently to the inelastic scattering processes, while they give a destructive coherence for the (t,p) process. In the limit $W_n(0,\lambda)\to 0$, $B(E\lambda;N_0(0\to\lambda))\to\infty$, while $\sigma(N_0\pm 2\ (\mathrm{g.s.})\to N_0(J^\pi=\lambda^\pi))\to 0$. Physically, this result is quite reasonable because two-body transfer cross sections probe particle-particle type of correlations while inelastic scattering processes probe particle-hole type of correlations. As pointed out in Ref. 18, the ground-state correlations induced by the λ-multipole particle-hole residual interaction and the λ-multipole pairing residual interaction destructively interfere. The understanding of the coexistence of both types of correlations is still an open and challenging question. Another problem that needs consideration is the possible double counting of the interactions, since $\sum_\mu P_{\lambda\mu}^\dagger P_{\lambda\mu}$ overlaps with $\sum_\mu Q_{\lambda\mu}Q_{\lambda\mu}^\dagger$ (see Sec. 4A).

III. COUPLING OF SINGLE-PARTICLE AND COLLECTIVE DEGREES OF FREEDOM

The coupling of a particle to a surface oscillation has received considerable attention. The usual coupling Hamiltonian depends linearly on the collective deformation parameter and the particle coordinates, and the radial form factor is peaked around the nuclear surface. In terms of the magnitudes defined in the previous section and making explicit use of Eq. (9), one obtains

$$h(0\lambda) = -\frac{\chi_\lambda}{2}\sum_\mu [(Q_{\lambda\mu})_{\rm coll} Q_{\lambda\mu}{}^\dagger + Q_{\lambda\mu}(Q_{\lambda\mu}{}^\dagger)_{\rm coll}], \tag{17}$$

where

$$(Q_{\lambda\mu})_{\rm coll} = -\frac{(2\lambda+1)^{1/2}}{\chi_\lambda}\sum_n \Lambda_n(0\lambda)[\beta_n{}^\dagger(0\lambda\,\mu) + (-1)^{\lambda-\mu}\beta_n(0\lambda-\mu)] \tag{18}$$

and

$$[(Q_{\lambda\mu})_{\rm coll}, Q_{\lambda\mu}{}^\dagger] = 0\,.$$

That is, the collective and particle degrees of freedom[19] are assumed to be independent but for the coupling [Eq. (17)]. The basic matrix elements are displayed in Fig. 2 and given in Appendix II.

The coupling Hamiltonian in the pairing case may also be derived from the basic Hamiltonian [Eq. (1)] and reads

$$h(2\lambda) = -G_\lambda 2\pi(2\lambda+1)\sum_\mu [(P_{\lambda\mu}{}^\dagger)_{\rm coll} P_{\lambda\mu} + (P_{\lambda\mu})_{\rm coll} P_{\lambda\mu}{}^\dagger], \tag{19}$$

where

$$P_{\lambda\mu}{}^\dagger = -\frac{1}{4\pi G_\lambda(2\lambda+1)^{1/2}}\sum_n [\Lambda_n(2\lambda)\beta_n{}^\dagger(2\lambda\,\mu) + (-1)^{\lambda-\mu}\Lambda_n(-2\lambda)\beta_n(-2\lambda-\mu)] \tag{20}$$

and

$$[(P_{\lambda\mu})_{\rm coll}, P_{\lambda\mu}{}^\dagger] = 0\,. \tag{21}$$

The basic matrix elements are displayed in Fig. 3 and Appendix II.

It is possible to define a dimensionless parameter, namely

$$t(\alpha\lambda) = \frac{\Lambda_n(\alpha\lambda)M(j_1 j_2;\lambda)_{\rm av}}{W_n(\alpha\lambda)}(2\lambda+1)^{1/2}, \tag{22}$$

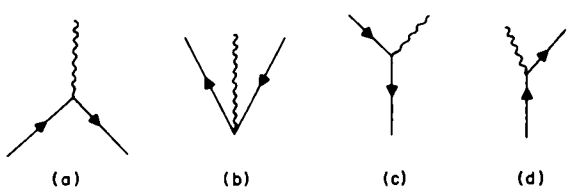

FIG. 2. Graphical representation of the four basic (first-order) matrix elements of the coupling Hamiltonian $h(0\lambda)$. The corresponding formulas are collected in Appendix II. The time is supposed to run upwards. A line which runs to positive values of time represents a particle while one running downwards represents a hole. The particle-hole collective mode (surface vibration) is represented by a wavy line. The interaction between particle (or hole) and the vibration takes place at the vertex, where parity, angular momentum, and number of particles must be conserved, although not energy.

where $M(j_1 j_2;\lambda)_{\rm av}$ is an average matrix element in the single-particle subspace considered. This parameter is equivalent to the parameter $t(0\lambda) = [(2\lambda+1)/16\pi](\hbar\omega/2C_\lambda)^{1/2}k/\hbar\omega_\lambda$ used in similar types of calculations.

The RPA matrix elements [Eqs. (8) and (16)] between zero and one-phonon states may be also obtained using the coupling Hamiltonians [Eqs. (17) and (19)] in first-order perturbation theory. The corresponding graphs are given in Fig. 4 together with the formal expression (see caption). Graph (a) represents the creation of two particles in the presence of the uncorrelated ^{208}Pb core and its subsequent coupling to build a pairing phonon, while graph (b) represents the annihilation of the two holes which are present in the correlated ground state. Similarly, graph (c) represents the creation of a particle-hole pair (ki). Subsequently the particle drops into the hole and sets the ^{208}Pb core in a surface (particle-hole) vibrational type of excitation. In graph (d) the independent particle-hole excitation and the vibrational phonon are present in the correlated ground state. At a later time the particle decays into the hole state. The external fields which are applied in each case are a $\alpha = 2$ field [graphs (a) and (b)] generated by a (t,p) reaction and a $\alpha = 0$ field [graphs (c) and (d)] generated by an inelastic proton reaction. Therefore, both the RPA treatment of the interaction [Eqs. (1) and (9)] and the perturbation treatment of Eqs. (17) and (19) are equivalent, i.e., they

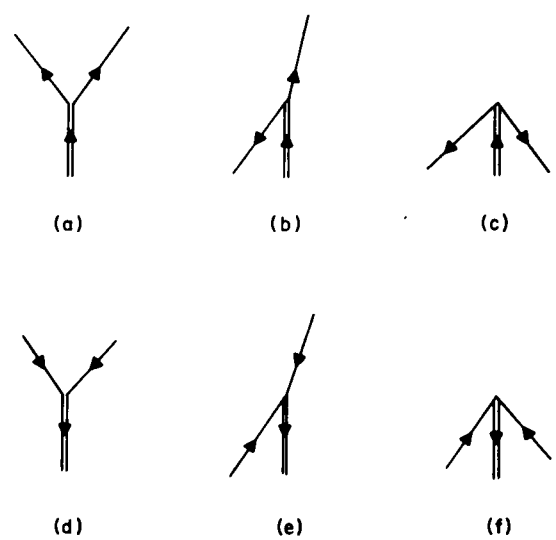

FIG. 3. Graphical representation of the basic (first-order) matrix elements of the coupling Hamiltonian $h(\pm 2\lambda)$. The same convention of particles and holes is used here as in Fig. 2 (see corresponding caption). In the present case, there are two possible modes of collective excitation for each spin and parity. Namely, the pair addition ($\alpha = 2$) and pair subtraction mode ($\alpha = -2$).

yield the same results concerning the specific operators matrix elements.

In the remainder of this paper, we carry out a perturbation treatment of the coupling Hamiltonians [Eqs. (17) and (19)]. However, we retain Eqs. (6) and (15) from the RPA approximation in order to determine the strengths $\Lambda_n(\alpha\lambda)$ from the experimental energies $W_n(\alpha\lambda)$.

IV. SPECTRUM OF ^{209}Pb

In this section we discuss the different steps necessary to calculate the two-particle–one-hole (2p-1h) spectrum of ^{209}Pb. Also the matrix elements of the one- and two-body transfer operators are derived.

A. Unperturbed Basic Set of States

The seven lowest states of ^{209}Pb correspond to "single-particle" states $|k\rangle$ dressed by the interaction with the cloud of phonons of the different types. The techniques developed in the present paper can be used directly to determine these physical single-particle states. However, we will not discuss them here.

The next states presumably represent 2p-1h states. To describe them, we use a subset of states consisting of a particle coupled to particle-hole phonon or a hole coupled to a pairing phonon

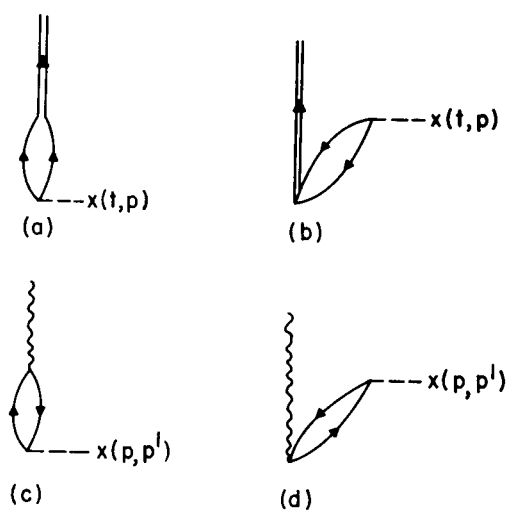

FIG. 4. Graphical representation of first-order [in the parameters $\Lambda_n(\alpha\lambda)$] matrix elements of the operators $[b_{j_1}^{\dagger}b_{j_2}^{\dagger}]_{\mu}^{\lambda}$ and $[b_k^{\dagger}b_i]_{\mu}^{\lambda}$ and their Hermitian conjugates between zero and one-phonon states. The values of the vertex corresponding to graphs (a)–(d) are listed in Appendix II, Eqs. (A2.5), (A2.7), (A2.1), and (A2.2), respectively. The energy denominators are equal to $-[\epsilon_{j_1}+\epsilon_{j_2}-W_n(\alpha\lambda)]$ for graphs (a) and (c), and to $[\epsilon_{j_1}+\epsilon_{j_2}+W_n(\alpha\lambda)]$ for graphs (b) and (d). The resulting expressions are thus equal to Eqs. (5) and (14).

with $\alpha=2$. That is, we construct the states in ^{209}Pb using elementary independent modes of ^{208}Pb which are assumed to be phonon excitations ($\alpha=0$, ±2) and particle (hole) excitations ($\alpha=\pm1$).

Correspondingly, the vacuum state is defined through $\beta_n(\alpha\lambda\mu)|0\rangle = b_k|0\rangle = b_i|0\rangle = 0$ and denotes the ^{208}Pb ground state.

The states belonging to our basic set will be labeled by $(n\alpha\lambda; j; JM)$, and, thus,

$$|n2\lambda; i; JM\rangle = [\beta_n^{\dagger}(2\lambda)b_i]_M^J|0\rangle\,,$$
$$|n0\lambda; k; JM\rangle = [\beta_n^{\dagger}(0\lambda)b_k^{\dagger}]_M^J|0\rangle\,. \tag{23}$$

B. Effective Interaction

Processes of first order in the interaction correspond, for example, to the stripping reaction on the closed-shell system leading to 2p-1h states (see Fig. 5). This type of process measures the ground-state correlations induced in the closed-shell system by the pairing on particle-hole vibrations and will be discussed elsewhere.[20]

In second order in the coupling strengths Λ, one obtains corrections to the single-particle energies as well as matrix elements of the Hamiltonian between our basic states. Because the energy difference between some of these states is small, we may need to diagonalize exactly the Hamiltonian within the basic set. Let us then define an effective Hamiltonian,

$$H_{\text{eff}} = \sum_{\nu} \frac{H|\nu\rangle\langle\nu|H'}{\Delta E_{\nu}}\,, \tag{24}$$

acting only within our basic set, i.e.,

$$\langle a|H_{\text{eff}}|b\rangle = \sum_{\nu} \frac{\langle a|H|\nu\rangle\langle\nu|H'|b\rangle}{\Delta E(\nu,a,b)}\,, \tag{25a}$$

$$\langle a|H_{\text{eff}}|\nu\rangle = 0\,, \tag{25b}$$

and where $H(H')$ can be either $h(0\lambda)$ or $h(2\lambda)$ defined in Eqs. (17) and (19). We denote by Latin letters the state belonging to our basic set, while Greek letters correspond to states belonging to the complementary space of states. We dis-

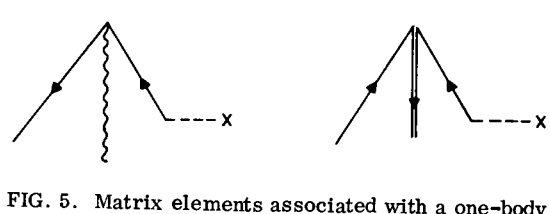

FIG. 5. Matrix elements associated with a one-body process of the type ^{208}Pb[(a) and (b)] ^{209}Pb(J^{π}), where ^{209}Pb(J^{π}), is a two-particle–one-hole state in ^{209}Pb described by the wave function given in Eq. (23). These stripping reactions can proceed only because of the existence of ground-state correlations, and the corresponding cross sections are a measure of them.

cuss now the form of the energy denominators $\Delta E(\nu, a, b)$. If we do perturbation theory with the effective Hamiltonian [Eq. (24)], the lowest and next-to-lowest order correction to the energy of the state $|a\rangle$ are

$$\omega_a^{(1)} = \langle a|H_{\text{eff}}|a\rangle = \sum_\nu \frac{\langle a|H|\nu\rangle\langle\nu|H'|a\rangle}{\Delta E(\nu, a, a)}, \tag{26}$$

$$\omega_a^{(2)} = \sum_b \frac{|\langle a|H_{\text{eff}}|b\rangle|^2}{\epsilon_a - \epsilon_b} = \sum_{b,\mu,\nu} \frac{\langle a|H|\nu\rangle\langle\nu|H'|b\rangle\langle b|H''|\mu\rangle\langle\mu|H'''|a\rangle}{(\epsilon_a - \epsilon_b)\Delta E(\nu, a, b)\Delta E(\mu, a, b)}. \tag{27}$$

Comparison of $\omega_a^{(1)}$ with the corresponding second-order expression for the original Hamiltonian H [Eqs. (17) and (19)] indicates that the denominator entering in the diagonal matrix element is $\Delta E(\nu, a, a) = \epsilon_a - \epsilon_\nu$. The denominator corresponding to the nondiagonal matrix elements $\Delta E(\nu, a, b)$ may be similarly obtained by comparing $\omega_a^{(2)}$ with the corresponding fourth-order expression for H. This is given by an expression similar to Eq. (27), where $\Delta E(\nu, a, b) = \epsilon_a - \epsilon_\nu$ is independent of the state b. Therefore, the construction of the matrix element [Eq. (25)] may proceed as follows[21]: We assume that in the final wave function there is a predominant amplitude corresponding to our basic state $|a\rangle$. Then all matrix elements have as denominator $\epsilon_a - \epsilon_\nu$,

$$\langle a|H_{\text{eff}}|b\rangle = \sum_\nu \frac{\langle a|H|\nu\rangle\langle\nu|H|b\rangle}{(\epsilon_a - \epsilon_\nu)}. \tag{28}$$

The diagonalization of this matrix amounts to do perturbation to all orders, with some restriction over intermediate sums. That is, the procedure outlined above has the advantage that, for each term in the series expansion of the energy in powers of H_{eff}, we obtain an equivalent term in the corresponding series expansion of H (aside from the fact that summations over some intermediate states are restricted within our basic subset of states when using H_{eff}). However, it has the disadvantage that each final state is obtained by diagonalizing a different matrix [since we change value of denominators in Eq. (25) according to which is the main unperturbed component in the final state]. Therefore, final states are in general not orthogonal to each other, sum rules do not need to be obeyed, etc.

An alternative procedure to calculate the denominators is to assume that our basic set consists of states which are much closer to each other than to any state $|\nu\rangle$. This is consistent with performing an exact diagonalization within the set $|a\rangle$. To the extent that $[(\epsilon_a - \epsilon_b)/(\epsilon_a - \epsilon_\gamma)] \ll 1$, we can use either $\epsilon_a - \epsilon_\nu$ or $\epsilon_b - \epsilon_\nu$ in Eq. (27) and, therefore, it is sensible as well to use the average $\Delta E(\nu, a, b) = \frac{1}{2}[(\epsilon_a - \epsilon_\nu) + (\epsilon_b - \epsilon_\nu)]$. This recipe for $\Delta E(\nu, a, b)$ yields a single matrix for all states having the same spin and parity, and therefore a set of orthogonal wave functions.

In calculating the energy denominators it is convenient to use, instead of $W_n(\alpha\lambda)$, the energy differences $\Delta W_n(\alpha\lambda)$ which are defined as

$$\begin{aligned} \Delta W_n(0\lambda) &= \epsilon_{g_{9/2}} - \epsilon_{p_{1/2}} - W_n(0\lambda), \\ \Delta W_n(2\lambda) &= 2\epsilon_{g_{9/2}} - W_n(2\lambda), \\ \Delta W_n(-2\lambda) &= 2\epsilon_{p_{1/2}} - W_n(-2\lambda). \end{aligned} \tag{29}$$

Therefore, $\Delta W_1(\alpha\lambda)$ measures the change in the energy provided by the residual interaction in the corresponding $(\alpha\lambda)$ channel considered.

The graphs corresponding to the construction of the effective Hamiltonian are displayed in Fig. 6. Graphs (e) to (h) have been discussed in recent papers. The explicit expression of these matrix elements are given in Appendix III.

Before discussing the transition probabilities it is important to mention that the chosen basis for describing ^{209}Pb is overcomplete. That is, there is a finite overlap (a) between states of type $|n2\lambda; i; IM\rangle$ and $|n0\lambda; k; IM\rangle$ and (b) within states $|n0\lambda; k; IM\rangle$. However, all states of type $|n2\lambda; i; IM\rangle$ are orthogonal among themselves.

An example of the nonorthogonality mentioned in case (a) is provided by the states $|1\rangle = |120; p_{1/2}; \frac{1}{2}m\rangle$ and $|2\rangle = |105; g_{9/2}; \frac{1}{2}m\rangle$. The main component of state $|1\rangle$ is $(1/\sqrt{2})\{[b_{g_{9/2}}{}^\dagger b_{g_{9/2}}{}^\dagger]^0 b_{p_{1/2}}\}^{1/2}|0\rangle$, while

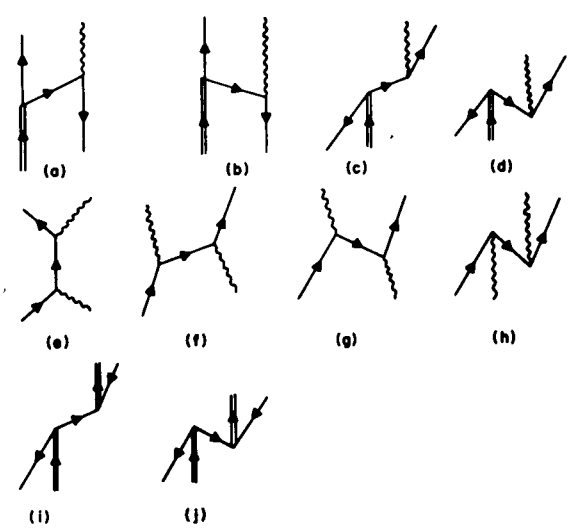

FIG. 6. Second-order contributions [in $\Lambda(\alpha\lambda)$ $(\alpha = 0, 2)$] to the matrix elements within the basic states describing the 2p-1h levels in ^{209}Pb [see Eq. (23)]. The explicit expressions of the corresponding matrix elements are given in Appendix III.

the main component of state $|2\rangle$ is

$$\{[b_{g_{9/2}}{}^{\dagger}b_{p_{1/2}}]^5 b_{g_{9/2}}{}^{\dagger}\}^{1/2}|0\rangle = -\sqrt{\tfrac{11}{20}}\{[b_{g_{9/2}}{}^{\dagger}b_{g_{9/2}}{}^{\dagger}]^0 b_{p_{1/2}}\}^{1/2}|0\rangle + \cdots .$$

The formalism reacts to this situation by presenting graphs (a) and (b) (Fig. 6) between states of type $|1\rangle$ and $|2\rangle$ and graphs (f) and (g) between states $|2\rangle$, but there is no graph of this class (i.e., with 2p-1h as intermediate state) having states of type $|1\rangle$ as initial and final state. Therefore, we must consider those graphs to be related to the lack of orthogonality of the basic set of states. In fact, the corresponding matrix elements include those 6-j coefficients necessary to find the overlap when the nonorthogonal states are expanded in terms of particle creation and annihilation operators, as indicated above.

C. Reaction Amplitudes

The perturbation method used in Sec. IV A to calculate the excitation energy of (2p-1h) states is used here to calculate the cross section for the population of these states in one- and two-particle transfer reactions. We analyze primarily the ^{207}Pb(t,p) and ^{210}Pb(p,d) reactions which give complementary information about the 2p-1h levels of ^{209}Pb. In what follows we discuss these transitions in different orders of perturbation in the coupling constants $\Lambda_n(\alpha\lambda)$.

In zero order, the only states of our basic set that can be populated in the single pickup reaction starting from $\beta_n{}^{\dagger}(20)|0\rangle$ (ground state of ^{210}Pb) are the states $|120; i; im\rangle$ [see Fig. 7(a)]. In the two-body stripping, we should only populate those states $|n2\lambda; p_{1/2}; im\rangle$ where $\beta_n{}^{\dagger}(2\lambda\mu)|0\rangle$ are those states of ^{210}Pb that are strongly excited in the ^{208}Pb(t,p) reaction. The experimental data provide a good verification of the lowest-order description, as it appears from the analysis done by Flynn *et al.*[22]

In second order in the coupling constants, we have corrections to Fig. 7(a) because the holes that move in ^{207}Pb are renormalized by its coupling to the collective phonons. That is, the states $|i\rangle$ spend part of the time in a state of 3p-2h [Figs. 7(b) and 7(e)] or 4p-3h [Figs. 7(c), 7(d), 7(f), and 7(g)], which effectively decreases the pickup cross section. Also in second order in $\Lambda_n(\alpha\lambda)$, the mixing of our basic states through the corresponding coupling Hamiltonians distributes the pickup strength over other states, whose main component is not excited in zero order. The wave functions of these states can be approximated by

$$|\nu, im\rangle_{\text{dressed}} = |\nu, im\rangle_{\text{bare}} + a\,|120; i; im\rangle , \qquad (30)$$

where $|\nu, im\rangle$ is a nonpickup state of angular momentum i. The transition rate associated with the *bare* pickup operator b_i leading to states of ^{209}Pb, having the same spin and parity as the single-hole states in ^{207}Pb, are proportional to $|a|^2$. These processes are graphically illustrated in the first and second column of Fig. 8. The initial state is $\beta_n{}^{\dagger}(200)|0\rangle$. The state $|120; i; im\rangle$ is created at some time t_1, and at a later time t_2 this state is perturbed by the effective interaction and goes into the final state.

To the same (second) order in the interaction constants $\Lambda_n(\alpha\lambda)$ there is another contribution to the pickup process. The corresponding graphs are displayed in the third column of Fig. 8. The single-hole state is created after the initial state is perturbed. In this way we see that the pickup operator has now a nonvanishing matrix element with all the final states (both $|n2\lambda; i_2; im\rangle$ and $|n0\lambda; k_2; im\rangle$ states) having the appropriate spin and parity. To include these last transitions in our formalism we must replace b_i by an *effective operator* $(b_i + B_i)$, where B_i has matrix elements given[23] in Appendix IV.

In the pickup process from ^{210}Pb to 2p-1h states having the same spin and parity as the single-

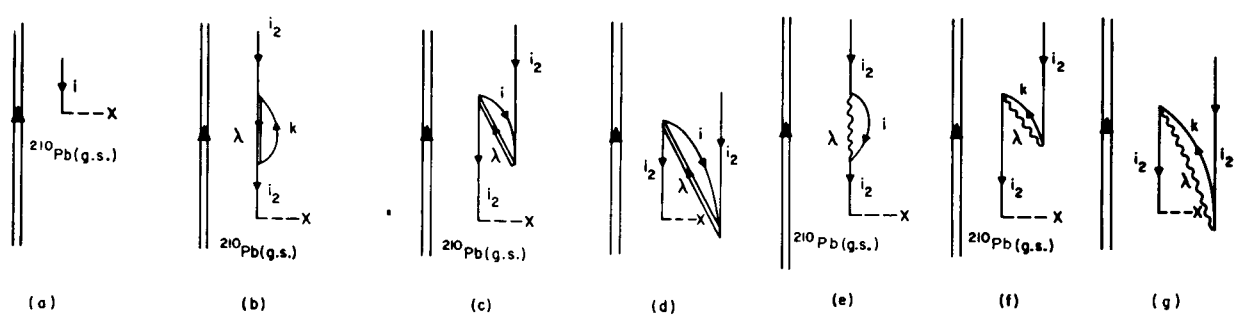

FIG. 7. Graph (a) displays the zeroth-order contribution in the coupling strength $\Lambda_n(\alpha\lambda)$ to the ^{210}Pb(p,d) reaction. In the rest of the figure, there are some of the second-order corrections to this cross section. These corrections take into account the fact that the hole states in ^{207}Pb are renormalized by the coupling to the collective phonons of ^{208}Pb (see text and Appendix IV).

particle states $b_k^\dagger|0\rangle$, there is no state within our basic set that can be populated in zero order. Therefore, the matrix elements of the corresponding *bare pickup operator* b_k are equal to zero, and all transitions take place through the B_k component of the *effective operator* $(b_k + B_k)$, which has matrix elements that are graphically displayed in Fig. 9 and given explicitly in Appendix IV.

In order to be consistent with the order in the strength $\Lambda_n(\alpha\lambda)$ up to which the pickup calculations to states $b_k^\dagger|0\rangle$ is performed, one should ignore all components in the wave function but the main state. Transitions through smaller admixtures are proportional both to matrix elements of B_k and to the matrix elements of Heff, and are, therefore, of fourth order in the interaction $h(\alpha\lambda)$ defined in Eqs. (17) and (19). Moreover, the main component has to be taken with amplitude 1, since any reduction from this value corresponds to normalization effects that are of sixth order in the coupling strengths.

The usual sum rules for transfer processes are modified by the perturbation treatment of the coupling between the odd neutron and the collective states of the core. For instance, using the equality

$$b_j b_j^\dagger + b_j^\dagger b_j = 1, \tag{31}$$

as in the work of Thouless,[24] we find that because ground-state correlations allow us to introduce a particle in a state below the Fermi surface, the sum rule for the one-body pickup process $(j = i)$ is now

$$\Sigma(i) = (2i+1)\sum_\psi |\langle\psi|b_i\beta_1^\dagger(200)|0\rangle|^2$$

$$= (2i+1)[1 - \sum_\phi |\langle\phi|b_i^\dagger\beta_1^\dagger(200)|0\rangle|^2], \tag{32}$$

where the states $|\phi\rangle$ belong to ^{211}Pb while $|\psi\rangle$ belongs to ^{209}Pb.

In first order of perturbation theory, only the states

$$|\phi_1\rangle \equiv \frac{1}{(1+\delta_{\lambda 0}\delta_{n1})^{1/2}}\,\beta_1^\dagger(200)\,|n2\lambda; i_2; im\rangle$$

and

$$|\phi_2\rangle \equiv \beta_1^\dagger(200)\,|n0\lambda; k; im\rangle$$

can be reached [see graphs (a) and (b) in Fig. 10], through an effective operator $B_i^\dagger$ having matrix elements

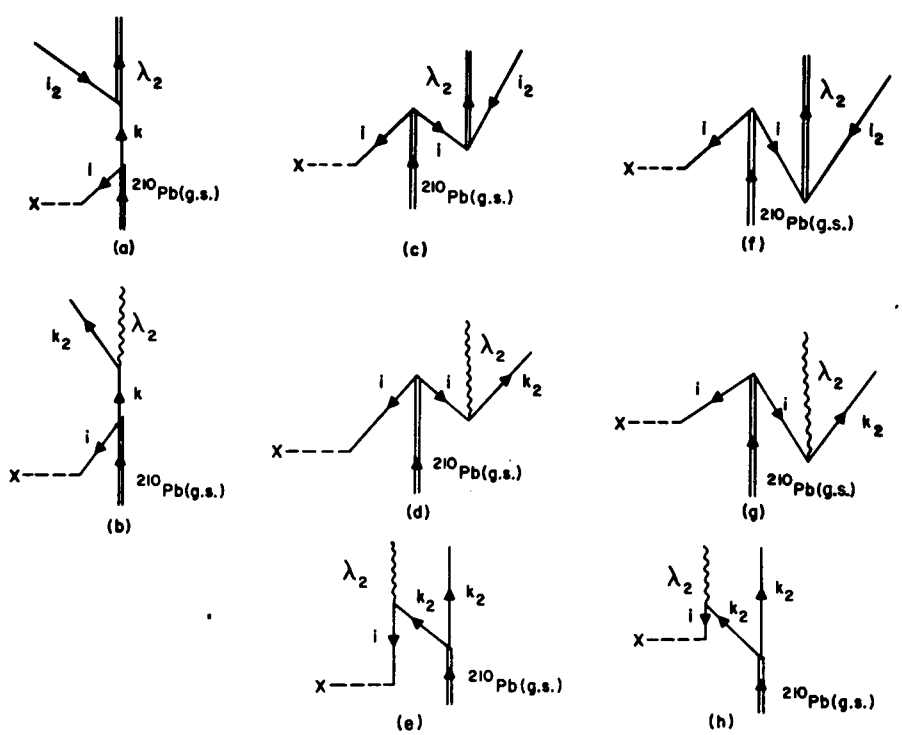

FIG. 8. Lowest-order graphs [in $\Lambda(\alpha\lambda)$] describing the pickup process ^{210}Pb$(p,d)^{209}$Pb(J^π), where J^π are 2p-1h unperturbed states of ^{209}Pb [see Eq. (23)]. In Fig. 8, the captured particle moves in the occupied states of the closed-shell system ^{208}Pb (i.e., in states denoted by i according to the convention adopted in Sec. II A).

$$\langle\varphi_1|B_i^\dagger\beta_1^\dagger(200)|0\rangle = \frac{1}{(2i+1)^{1/2}}\Lambda_n(2\lambda)(2\lambda+1)^{1/2}(1+\delta_{\lambda 0}\delta_{n1})^{1/2} \times \frac{M(i_1 i_2;\lambda)}{2\epsilon_{g_{9/2}} - \epsilon_{i_2} - \epsilon_i - \Delta W_n(2N)}, \tag{33}$$

$$\langle\varphi_2|B_i^\dagger\beta_1^\dagger(200)|0\rangle = \frac{1}{(2i+1)^{1/2}}\Lambda_n(0\lambda)(2\lambda+1)^{1/2} \times \frac{M(ik;\lambda)}{\epsilon_k + \epsilon_{g_{9/2}} - \epsilon_i - \epsilon_{p_{1/2}} - \Delta W_n(0\lambda)}. \tag{34}$$

If we put $j=k$ in Eq. (31), the sum rule corresponding to Eq. (32) is

$$\Sigma(k) = \sum_\phi |\langle\phi|b_k^\dagger\beta_1^\dagger(200)|0\rangle|^2 = 1 - \sum_\psi |\langle\psi|b_k\beta_1^\dagger(200)|0\rangle|^2 \tag{35}$$

and refers to the one-body stripping reaction from ^{210}Pb to states ϕ in ^{211}Pb. The states $|\psi\rangle$ entering in Eq. (35) belong to ^{209}Pb. Then, the SR for the case of the ^{210}Pb(p,d) reaction under study would be the correction given by the second term in Eq. (35). However, in lowest order, the states contain two phonons [see graphs (c) and (d)] and do not belong to our basic set. We have to go up to the fourth-order correction to the SR given by Eq. (35) (second term) to get any number related to the pickup process leading to our basic states. We then see that in this case the second-order SR limit [Eq. (35)] is not directly relevant to our calculation.

A similar discussion applies to the two-body transfer operator. In zeroth order, the operator $T^{(0)}_{\lambda\mu}(j_1,j_2) = [b_{j_1}^\dagger b_{j_2}^\dagger]^\lambda_\mu$ gives zero spectroscopic amplitudes for the transitions between the ground state of ^{207}Pb$(b_{p_{1/2}}|0\rangle)$ and states belonging to our basic set. The lowest nonvanishing contribution is obtained in first-order perturbation theory. These processes are represented graphically in Fig. 11 and the corresponding spectroscopic amplitudes are given in Appendix V. We notice that in Figs. 11(a) and 11(b), the hole state is inactive during the entire process. These two figures (in the absence of the hole line) represent the transitions from ^{208}Pb to ^{210}Pb, and therefore may correspond to very enhanced processes. In fact, the corresponding matrix elements (A5.1) and (A5.2) [divided by $(1+\delta_{12})^{1/2}$] are identical to those given in Eq. (8).

There are two types of third-order transitions, one that proceeds through the *first-order effective transfer operator* $T^{(1)}_\lambda(j,j')$ and excites the small (second-order) components of the state in question, and another that is proportional to the matrix element of the *third-order effective operator* $T^{(3)}_\lambda(j,j')$ and excites directly the main component. In Fig. 12 we illustrate one of these processes. As can be seen, the cross sections associated with transitions of type (a) are going to be systematically larger than those corresponding to graph (b) as the energy denominators entering in (a) are smaller than those of (b).

As no higher order than the first was explicitly considered in evaluating the two-body stripping spectroscopic amplitude, all third- and higher-order effects that are included through the diagonalization procedure are of the type (a), which is consistent with our previous discussion.

V. DETERMINATION OF THE PARAMETERS ENTERING IN THE CALCULATION

In order to proceed with the calculation we must decide upon the shape of the radial function $f_\lambda(r)$ entering in the matrix elements $M(j_1 j_2;\lambda)$ defined in Eq. (2e). Because we are treating a surface phenomena, we expect $f_\lambda(r)$ to be peaked around the nuclear surface. This is conveniently achieved if we use a radial form factor $f_\lambda(r)$ proportional to the derivative of the Woods-Saxon potential with respect to r. An alternative method is to use $f_\lambda(r) = r^\lambda$, which does not yield significant deviations

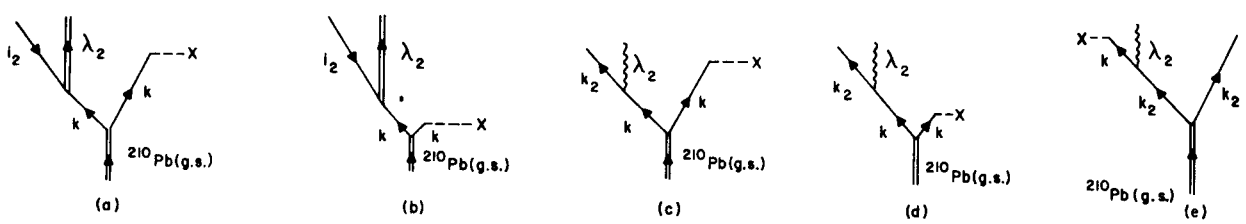

FIG. 9. Lowest-order graphs [in $\Lambda(\alpha\lambda)$] describing the pickup process ^{210}Pb$(p,d)^{209}$Pb(J^π), where J^π are 2p-1h unperturbed states of ^{209}Pb [see Eq. (23)]. The captured particle moves in the empty states of the closed-shell system ^{208}Pb (i.e., states denoted by k in the text; see Sec. II A). The explicit expression of the matrix elements is given in Appendix IV.

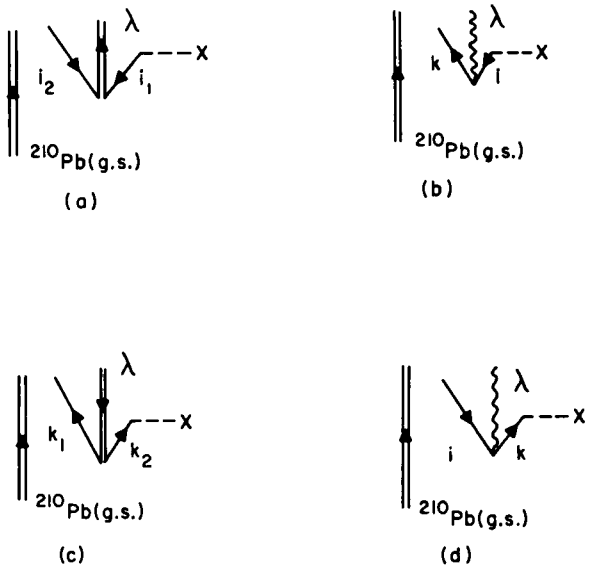

FIG. 10. Graphical representation of the matrix elements associated with perturbative corrections [in $\Lambda_n(\alpha\lambda)$] to the sum rule for one-body stripping and pick-up processes starting from ^{210}Pb(g.s.).

from the former radial dependence, as long as we consider single-particle states having similar mean square radius. This situation is obtained by considering only seven single-neutron and six single-proton states above the Fermi surface, and the same number below.

In principle we do not need to have the same radial dependence for both the $\alpha=0$ and the $\alpha=\pm2$ matrix elements, but we have chosen them to be equal throughout this paper.

To determine the boson parameters [the energies $W_n(\alpha\lambda)$ and the coupling strength $\Lambda_n(\alpha\lambda)$] we use the first of the methods outlined in Sec. II A, i.e., we input into the RPA Eqs. (6) and (15) the experimental energy corresponding to the lowest state carrying angular λ and parity $\pi=(-1)^\lambda$. Thus we obtain values for G_λ and χ_λ, which are displayed in Table I.

It is interesting to point out that the resulting wave functions, when used to calculate the reduced transition probabilities $B(E\lambda;0\to\lambda)$ in ^{208}Pb or the spectroscopic amplitudes associated with the ^{208}Pb$(t,p)^{210}$Pb reaction, give results that are in good agreement with experiment (see Tables II and III). In the case of phonons with transfer quantum number $\alpha=\pm2$, we obtain two values for each G_λ, corresponding to whether we use the lowest state of angular momentum λ in ^{210}Pb or in ^{206}Pb. It turns out that, systematically, the strength resulting from the $\alpha=+2$ boson is smaller than the one arising from the $\alpha=-2$ boson. This may be partially due to the fact that the harmonic-oscillator central potential overestimates the radial difference between states moving above and below the Fermi surface. We have thus attenuated the radial dependence of the matrix element between states 1, 2 by multiplying $\langle 1|r^\lambda|2\rangle$ by a coefficient of the form

$$Z_{12}=\frac{2\langle 5l|r^2|5l\rangle}{\langle N_1l_1|r^2|N_1l_1\rangle+\langle N_2l_2|r^2|N_2l_2\rangle}=\frac{13}{N_1+N_2+3}, \tag{36}$$

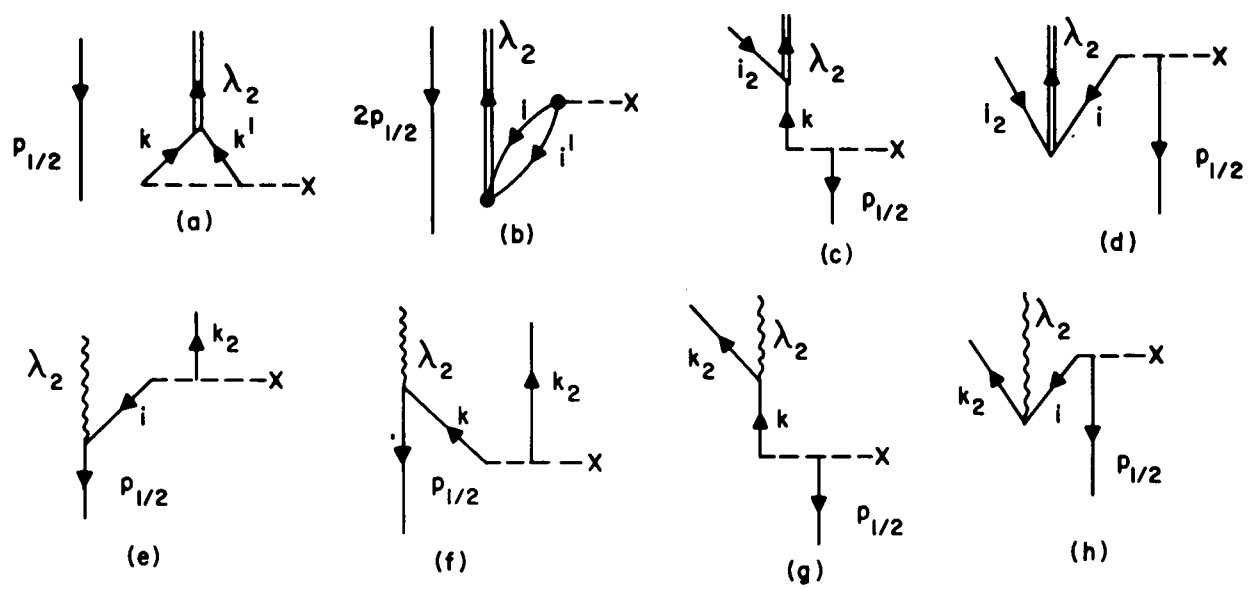

FIG. 11. Lowest-order graphs in $[\Lambda_n(\alpha\lambda)]$ describing the different contributions to the ^{207}Pb$(t,p)^{209}$Pb(J^π) reaction exciting the basic 2p-1h states [see Eq. (23)] of ^{209}Pb. Graphs (a) and (b) (apart from the inert $p_{1/2}$ hole state) describe the ^{208}Pb$(t,p)^{210}$Pb reaction. The corresponding expressions are listed in Appendix V.

where N is the principal oscillator quantum number. We notice empirically that using a similar factor for all λ, the two values of G_λ become very close (see Table I). The average $G_\lambda(A-2)$ and $G_\lambda(A+2)$ is used finally in order to determine $\Lambda_n(\alpha\lambda)$ and $W_n(\alpha\lambda)$ corresponding to the higher roots of the RPA equations.

The parameters thus obtained depend critically on the distances between the lowest unperturbed poles and the experimental energies (see Table I and Fig. 1). This number is very small for the 6^+ and 8^+ states in ^{210}Pb and, moreover, is obtained as a difference between much larger numbers. Therefore, we have taken W_1 and ΔW_1 from theoretical calculation of Redlich.[25] In the case of the 8^+ phonon, the value of G_8 is determined only from the $\alpha=+2$ phonon, as no data on 8^+ states are available in the case of ^{206}Pb.

A completely similar calculation is done for the case of the $\alpha=0$ particle-hole phonons. Although now only one value of χ_λ appears for each λ, we have kept the correction given by Eq. (36) in the radial matrix elements. The parameters for the lowest roots are also given in Table I. It is interesting to point out that there is no free parameter in this description of the coupling of a particle to a vibration, and that the mixing between the basic states is determined by the experimental energies of the $\alpha=0$ and ±2 phonons.

The next step is to decide which bosons are to be included in the calculation. As mentioned in Sec. VI B, the perturbation method takes care of the overcompleteness of the basic set of states (to the order of the applied perturbation). However, from the point of view of perturbation theory, the diagonalization procedure implies that we are taking some effects up to higher order than others and, therefore, the corrections arising from overcompleteness may not be done properly. Especially large matrix elements arise from graphs (a), (b), (f), and (g) of Fig. 6 when, for instance, the particle-hole phonon is close to a pure particle-hole configuration [such as the lowest 5^- particle-hole phonon at 3.2 MeV whose main component is the $(g_{9/2},p_{1/2}^{-1})$ configuration with unperturbed energy 3.41 MeV]. In principle, for these cases, we should carry to a higher order the calculation of the effective Hamiltonian. However, this program is difficult to work out. We have preferred not to include in the calculation those particle-hole phonons which have a dominant single particle-hole component. Therefore, we have kept the lowest 3^- state at 2.6 MeV as the only ($\alpha=0$) phonon. As $\alpha=-2$ and +2 phonons, we have included the lowest phonon states of ^{206}Pb and ^{210}Pb with $\lambda=0^+$, 2^+, 4^+, 6^+, and 8^+. In some occasions, namely to study levels at about 4 MeV of excitation energy in ^{209}Pb, we have also included higher-energy particle-particle and hole-hole phonons. The parameters characterizing the extra phonons are given in Table IV.

The single-particle energies were taken from the experimental single-particle and single-hole levels in ^{209}Pb, ^{209}Bi, ^{207}Pb, and ^{207}Tl.[26]

VI. DISCUSSION OF THE RESULTS

In order to discuss the agreement between predicted and experimental numbers we should sort out the cases that may be meaningfully used for comparison. For instance, in the case of the $I^\pi=\frac{1}{2}^-$ states, neither experiments nor theory indicate that levels other than the one having as main component the $|120;p_{1/2};1/2M\rangle$ states are populated in both the two-body stripping and the one-body pickup reactions [see Table V(a) of the following paper]. Therefore, this agreement between theory and experiment is not significant evidence in favor of our calculation, since the zero-order approximation (see Fig. 7) yields the same result. The same can be said about states having the same spin and parity as the single-particle states in

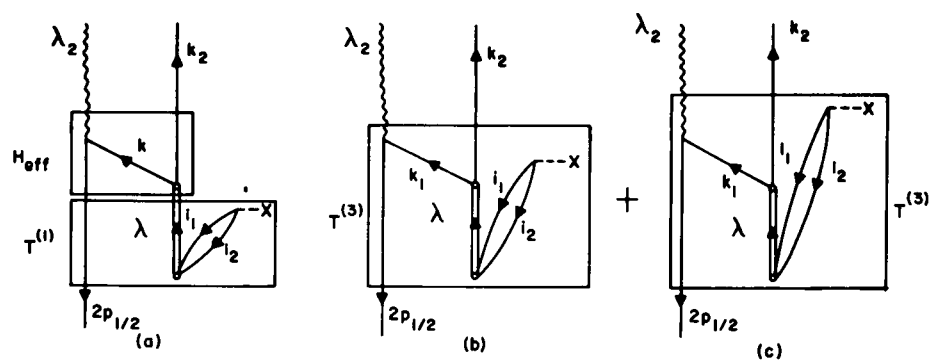

FIG. 12. Example of a third-order contribution to the two-body transfer process [^{207}Pb$(t,p)^{209}$Pb], exciting a 2p-1h state of the basic set [Eq. (23)].

TABLE III. Reduced electromagnetic transition probabilities associated with low-lying one-phonon collective particle-hole states of ^{208}Pb($|1(0\lambda)\rangle$). The wave functions used for describing these phonon states are given in Eq. (14) and the values of the parameters chosen were those of Table I. The multipole operator is defined as $M(E\lambda)=\sum_k\{e[\frac{1}{2}-t_z(k)]+(e_{\rm pol})_{E\lambda}\}r_k^\lambda Y_{\lambda\mu}(\theta_k,\phi_k)$ [see A. Bohr and B. R. Mottelson, *Nuclear Structure* (W. A. Benjamin, Inc., New York, 1969), Vol. 1]. In the second and third columns, the reduced matrix element of the operator $r^\lambda Y_{\lambda\mu}$ is given both for the proton and the neutron component of the wave function, respectively. In the fourth column, the value $(e_{\rm pol})_{E\lambda}$ is given which is used to reproduce the experimental results listed in the fifth column. In the last column, the experimental cross sections are given in terms of single-particle units defined as $B(E\lambda;\ 0\to\lambda)_{\rm sp}=[(2\lambda+1)/4\pi]\{[3/(3+\lambda)]eR_0^\lambda\}^2$.

	$\langle 0\|\|r^\lambda Y_\lambda\|\|1(10\lambda)\rangle\left(\frac{\hbar}{Mw}\right)$				
λ^π	Protons	Neutron	$(e_{\rm pol})_{E\lambda}$	$B(E\lambda;\ 0\to\lambda)$ [e^2 (10^{-24} cm^2)$^\lambda$]	$\frac{B(E\lambda;\ 0\to\lambda)}{B_{\rm sp}}$
2^+	1.93	3.54	0.40	0.30 [a]	8.0
3^-	13.6	28.2	0.13	0.53 [b]	31.5
5^-	25.4	127.4	1.30	0.04 [c]	10.7

[a] F. G. Ziegler and G. A. Peterson, Phys. Rev. 165, 1337 (1968).
[b] A. R. Barnett and W. R. Phillips, Phys. Rev. 186, 1205 (1969).
[c] A. Scott and M. Fricke, Phys. Letters 20, 1675 (1966).

^{209}Pb (for example, the $J^\pi=\frac{9}{2}^+$, $\frac{11}{2}^+$, etc. states). The largest (p,d) spectroscopic factor we predict for these states (we leave out of the present discussion the $\frac{15}{2}^-$ states) is 1.2% to the $J^\pi=\frac{9}{2}^+$ level at 4.21 MeV. The zero-order prediction is $S=0$ and, therefore, the theoretical predictions are again rather independent of the approximation. There is no evidence that any of such states are excited in the pickup process.

From the preceding discussion we conclude that, in order to discuss the one-particle pickup, we should look at the $\frac{3}{2}^-$, $\frac{5}{2}^-$, $\frac{7}{2}^-$, and $\frac{13}{2}^+$ states. In all these cases most of the reaction strength is concentrated at a definite energy [see Table V of the present paper and also Table V(b), V(c), V(d), and V(p) of Ref. 8]. This energy agrees reasonably well with the experimental number, but again this is true in the zeroth-order approximation. However, the spectroscopic factors for the (p,d) reaction agree with the theoretical predictions only after the diagonalization has been made.

In addition to the main cross sections listed in Table V, we predict also an appreciable (p,d) intensity to the lowest $\frac{3}{2}^-$, $\frac{5}{2}^-$, and $\frac{7}{2}^-$ state [see Table V(b)–V(d) of Ref. 8]. The main component of these states is $|103;g_{9/2};IM\rangle$ and, *therefore*, the one-body pickup strength associated with these levels is built from contributions of graphs (e) and (h) of Fig. 8. The experimental spectroscopic factors are also rather large, and are well reproduced by the theoretical calculations in the $\frac{3}{2}^-$ and $\frac{5}{2}^-$ cases. The corresponding state for the $\frac{7}{2}^-$ case has not been clearly identified, although there is a state at 2.563 MeV which is populated in an $l=3$ transition and for which we cannot find a partner among the predicted states with $I^\pi=\frac{5}{2}^-$.

We saw before that the agreement of the predicted spectroscopic factors for the (p,d) reaction exciting states whose main component is $|120;i;im\rangle$ with experiment is good (see Table V). We can

TABLE IV. RPA parameters associated with excited $\alpha=\pm2$ phonon states (see caption to Table I).

		0_2^+	0_3^+	0_4^+	2_2^+	2_3^+	2_4^+	4_2^+	4_3^+
^{208}Pb	$\Lambda_n(2\lambda)$ [$(Mw/\hbar)^{\lambda/2}$ MeV]	0.85	0.62	0.16	0.45×10^{-1}	0.61×10^{-1}	0.12×10^{-2}	0.29×10^{-2}	0.51×10^{-2}
	$W_n(2\lambda)$ (MeV)	2.16	3.61	4.31	1.94	2.11	2.79	1.98	2.39
^{206}Pb	$\Lambda_n(-2\lambda)$ [$(Mw/\hbar)^{\lambda/2}$ MeV]	0.98	0.45	0.79	0.27×10^{-1}	0.19×10^{-1}	0.17×10^{-1}	0.28×10^{-1}	0.28×10^{-2}
	$W_n(-2\lambda)$ (MeV)	1.07	2.21	3.31	1.43	1.72	2.08	1.95	2.85

		4_6^+	6_2^+	6_3^+	6_4^+	8_2^+	8_3^+	8_4^+
^{208}Pb	$\Lambda_n(2\lambda)$ [$(Mw/\hbar)^{\lambda/2}$ MeV]	0.14×10^{-3}	0.30×10^{-3}	0.40×10^{-3}	0.14×10^{-3}	0.24×10^{-4}	0.20×10^{-4}	0.31×10^{-4}
	$W_n(2\lambda)$ (MeV)	2.83	1.91	2.48	2.81	1.83	2.70	3.05
^{206}Pb	$\Lambda_n(-2\lambda)$ [$(Mw/\hbar)^{\lambda/2}$ MeV]	0.24×10^{-2}	0.11×10^{-3}	0.14×10^{-3}	0.16×10^{-3}	0.18×10^{-4}	0.47×10^{-5}	0.17×10^{-4}
	$W_n(-2\lambda)$ (MeV)	3.47	3.82	4.59	4.88	6.37	7.62	10.21

then rely on the predicted spectroscopic factor for states whose main component is $|103;g_{9/2};IM\rangle$ as these states are excited in the pickup reaction through the admixtures with the $|120;i;im\rangle$ states. It may be thus possible to locate many of the levels belonging to the septuplet ($\frac{3}{2} \leq I \leq \frac{15}{2}$). It is interesting to compare (a) our results with the predictions of Hammamoto[7] who used a similar model in which she focuses the attention on the particle-hole 3^- phonon and only estimates roughly the influence of the hole coupled to the ground state of ^{210}Pb and (b) the splitting of the septuplet in ^{209}Bi and ^{209}Pb (Table VI). Both theoretical calculations yield similar results for ^{209}Pb, and they are also in good agreement with the experimental results.

In addition to the transitions populating the previously discussed levels, other states are also populated in the one-body pickup processes [see Tables V(b)–V(d) of the following paper[8]]. Among these states there is, in both the $\frac{3}{2}^-$ and $\frac{5}{2}^-$ cases, at least one state that is strongly populated also in the ^{207}Pb$(t,p)^{209}$Pb reaction and, *therefore*, has to be mainly the $|122;p_{1/2};IM\rangle$ state. Both theory and experiment agree in a pickup spectroscopic factor of 0.20 for the population of the corresponding $\frac{3}{2}^-$ state. In the $\frac{5}{2}^-$ case there are two states seen in the (t,p) reaction where the model predicts only one (the state at 2.98 MeV). The (p,d) spectroscopic factor of this state (found experimentally at 2.873 MeV) is an order of magnitude larger than the predicted one [see Table V(c) of Ref. 8]. In lowest (second) order, the population of these states is made through graphs (c) and (f) of Fig. 8. Because matrix elements with the same numerator correspond to both figures, the ratio of the matrix elements is simply given by the ratio of denominators, namely

$$\frac{\langle 122;i_2;im|b_i\beta_1^\dagger(200)|0\rangle_{\text{graph (c)}}}{\langle 122;i_2;im|b_i\beta_1^\dagger(200)|0\rangle_{\text{graph (f)}}} = -\frac{\epsilon_{p_{1/2}} - \epsilon_{i_2} + W_1(22) - W_1(20)}{\epsilon_{i_2} + \epsilon_{p_{1/2}} + W_1(22)}, \tag{37}$$

where $W_1(22) - W_1(20) = 0.795$ MeV is the excitation energy of the lower 2^+ state in ^{210}Pb (see Table I). We see that both matrix elements will be coherent in the case of $i^\pi = \frac{3}{2}^-$ state ($\epsilon_{p_{1/2}} - \epsilon_{p_{3/2}} = 0.90$ MeV $> W$), while they will be incoherent for $i^\pi = \frac{5}{2}^-$ ($\epsilon_{p_{1/2}} - \epsilon_{f_{5/2}} = 0.57$ MeV $< W$). Therefore, it is difficult to increase the (p,d) spectroscopic factor of the $\frac{5}{2}^-$ 2.98-MeV state and at the same time to decrease the spectroscopic factor of the 2.79-MeV state. This would mean to mix more strongly the unperturbed $|122;p_{1/2};\frac{5}{2}m\rangle$ and $|120;f_{5/2};\frac{5}{2}m\rangle$ states without affecting the agreement obtained for the $\frac{3}{2}^-$ states. The increase of the mixing mentioned above would also distribute the (t,p) strength between the two $\frac{5}{2}^-$ states. Several attempts have been made to check whether it is possible to improve this situation:

(1) Increase the strength of the coupling constant. If we multiply all coupling constants Λ by the same factor, there is an unacceptable over-all decline of the agreement with the energies and the previously discussed transition rates, before the $|122;p_{1/2};\frac{5}{2}m\rangle$ and $|120;f_{5/2};\frac{5}{2}m\rangle$ unperturbed states become mixed to the extent that is needed in order to reproduce the experimental numbers. As the previous agreement depends largely on the coupling strengths $\Lambda_1(20)$ and $\Lambda_1(03)$, we checked the effect of multiplying by 2 all other coupling strengths but the previous two. No significant improvement was obtained in this way either.

(2) Change the single-particle energy of the $f_{5/2}$ state. One needs an increase of about 200 keV in the distance between this state and the $p_{1/2}$ single-particle level to obtain the desired mixing. However, calculation of different renormalization effects which may lead to this shift of single-particle energies failed to yield such a displacement.

(3) Finally, our coupling Hamiltonian may be insufficient to describe adequately the mixing of states. We have tested the adequacy of the model concerning the mixing of unperturbed $|103;g_{9/2};im\rangle$ and $|120;i;im\rangle$ states. This mixing proceeds through graphs (a), (b), (c), and (d) of Fig. 6, among which the contribution of the first two is much larger than that corresponding to the last ones. Now, the mixing of the $|122;p_{1/2};im\rangle$ and $|120;i;im\rangle$ states proceeds in our model only through the relative small contribution (j) of Fig. 6 [which is of the same order of the (c) and (d) of

TABLE V. In the first two rows we list the zero-order predictions of the particle-vibration-coupling model concerning the energy and one-body pickup spectroscopic factor for the same 2p-1h states of ^{209}Pb. In the fifth and sixth rows are collected the corresponding predictions of the model taking into account the coupling. The experimental data (Ref. 8) are displayed in rows 3 and 4. In the last row we give the sum-rule limit as defined in Eq. (32).

J^π	$\frac{1}{2}^-$	$\frac{3}{2}^-$	$\frac{5}{2}^-$	$\frac{7}{2}^-$	$\frac{13}{2}^+$
$E^{(0)}$	2.17	3.07	2.77	4.52	3.81
$S^{(0)}$	2	4	6	8	14
E_{exp}	2.15	3.08	2.74	4.25	3.66
S_{exp}	2.15	2.62	4.76	5.34	11.80
E	2.22	3.19	2.79	4.56	3.83
S	1.83	2.60	5.21	5.15	12.59
Σ	1.83	3.71	5.62	7.75	13.74

TABLE VI. Theoretical predictions for the energies (measured from the 2.62-MeV octupole vibration of ^{208}Pb) and spectroscopic factors of the septuplet of levels $|103; g_{9/2}; jm\rangle$ in ^{209}Pb. The experimental results are also displayed. In the first two rows the energies of the septuplet of states $|103; h_{9/2}; j^+\rangle$ in ^{209}Bi is displayed for comparison, together with the corresponding experimental data.

		$\frac{3}{2}$	$\frac{5}{2}$	$\frac{7}{2}$	$\frac{9}{2}$	$\frac{11}{2}$	$\frac{13}{2}$	$\frac{15}{2}$
^{209}Bi	E Theory [a]	0	−10	9	−125	−43	−88	218
	Experiment [b]	−128	−4	−37	−56	−20	−20	122
^{209}Pb	E Theory [a]	−250	−270	44	−160	−2	−132	80
	Theory [c]	−260	−250	−20	−150	58	−120	850
	Experiment [d]	−300	−157	−57		−13 [e]		940
	S Theory [c]	1.21	0.51	0.13	0.00	0.00	0.00	0.09
	Experiment [d]	0.50	0.60	(0.02)				Weak

[a] See Ref. 7.

[b] R. A. Broglia, J. Lilley, R. Perazzo, and B. Phillips, Phys. Rev. C 1, 1508 (1970).

[c] Present calculation.

[d] See Ref. 8.

[e] This state is not seen in Ref. 8 and was assigned in Ref. 7.

the previous case]. The discrepancy found in the $\frac{5}{2}^-$ case thus is that the contribution (j) alone is not sufficient.

We notice that the usual quadrupole particle-hole force will indeed provide for a coupling between these two states.[27] In order to include this effect in the Hamiltonian we should add to Eq. (19) terms with two boson creation operators such as

$$\sum_{\mu}[\beta_{n_1}{}^{\dagger}(2\lambda_1)\beta_{n_2}(2\lambda_2)]^{\lambda}_{\mu}P_{\lambda\mu}\,. \tag{38}$$

We plan to study in the future the influence of such terms, both in the spectrum of odd and even nuclei. We give in Fig. 13 a schematic representation of the coupling term [Eq. (38)].

At higher energy there are states with $I^{\pi} = \frac{3}{2}^-$, $\frac{7}{2}^-$, and $\frac{13}{2}^-$ which are again populated in the (p,d) reaction with a spectroscopic factor which is typically an order of magnitude larger than the ones predicted by the model. It is possible that also in this case the coupling [Eq. (38)] may be adequate to explain these transitions.

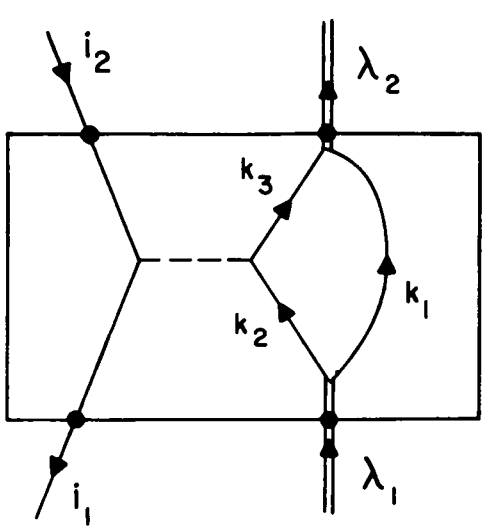

FIG. 13. Graphical representation of the coupling term given in Eq. (39).

Because the matrix element

$$\langle j_{15/2}|h(03)|103;g_{9/2};\tfrac{15}{2}\rangle$$

is very large, one can excite $\frac{15}{2}^-$ states in the ^{210}Pb-(p,d) reaction through processes represented by graphs (c) and (d) of Fig. 9, where $k = j_{15/2}$, $k_2 = g_{9/2}$, and $\lambda_2^{\pi} = 3^-$. We predict that the lowest $\frac{15}{2}^-$ state at 3.22 MeV, which is mainly $|103;g_{9/2};\frac{15}{2}\rangle$ [see Table V(g) of the following paper], will have a spectroscopic factor of 6%. Experimentally the state at 3.561 MeV is a possible candidate for this assignment.

We give in Table V of the next paper the modified sum rules for pickup as obtained from Eq. (32). In all cases $[(2i+1) - \mathrm{SR}(i)]/(2i+1) \lesssim 0.1$ [see Table V(a)–V(f) and V(n) of Ref. 8].

Finally in Table VII we display a comparison between the results obtained using the two possible sets of energy in the construction of the effective coupling Hamiltonian (Sec. IV B). No significant differences appear between them. In all the tables but Table VII, the second recipe, corresponding to an average between the energy of the initial and final states, is used.

VII. CONCLUSIONS

The most relevant conclusion of the present (and following) paper is that, in closed-shell nuclei plus (minus) one particle, the description of states at excitation energies from 2 to 4 MeV in terms of the superposition of elementary excitations appears to be both possible and useful. These elementary excitations of the same and

TABLE VII. Energy, single-particle pickup spectroscopic factor, and more relevant amplitudes $a(n_{\alpha\lambda}; j; JM)$ associated with the lowest (2p-1h) $J^\pi = \frac{1}{2}^-$, $\frac{3}{2}^-$, and $\frac{5}{2}^-$ states of ^{209}Pb. The difference between results I and II is that in I average energy denominators have been used to construct the effective Hamiltonian, whether in II the prescription suggested by perturbation theory is adopted (see Sec. IV B).

	I			II		
			$J^\pi = \frac{1}{2}^-$			
E(MeV)	2.22	3.57	3.82	2.22	3.54	3.73
S	1.83	0.00	0.00	1.89	0.00	0.00
$a(120; p_{1/2}; \frac{1}{2})$	1.00	0.03	0.01	1.00	0.01	0.01
			$J^\pi = \frac{3}{2}^-$			
E(MeV)	2.36	2.98	3.19	2.23	2.98	3.15
S	1.21	0.20	2.60	1.63	0.11	3.06
$a(122; p_{1/2}; \frac{3}{2})$	−0.11	0.97	0.20	−0.006	0.98	0.17
$a(222; p_{1/2}; \frac{3}{2})$	−0.03	0.01	0.03	−0.01	0.00	−0.02
$a(322; p_{1/2}; \frac{3}{2})$	−0.05	0.02	0.04	−0.02	−0.01	−0.02
$a(103; g_{9/2}; \frac{3}{2})$	0.91	0.03	0.29	0.88	0.01	0.20
$a(120; p_{3/2}; \frac{3}{2})$	0.32	0.23	−0.91	0.41	0.18	−0.96
			$J^\pi = \frac{5}{2}^-$			
E(MeV)	2.37	2.79	2.98	2.32	2.78	2.98
S	0.51	5.21	0.08		5.40	0.02
$a(122; p_{1/2}; \frac{5}{2})$	−0.04	−0.14	0.99	−0.03	−0.12	0.98
$a(222; p_{1/2}; \frac{5}{2})$	−0.01	−0.01	−0.01	−0.01	−0.01	0.00
$a(322; p_{1/2}; \frac{5}{2})$	−0.02	−0.01	−0.01	−0.01	−0.01	−0.01
$a(103; g_{9/2}; \frac{5}{2})$	−0.96	−0.19	−0.07	−0.94	−0.14	−0.06
$a(120; f_{3/2}; \frac{5}{2})$	−0.20	−0.96	0.12	−0.26	0.97	0.05

neighboring nuclei are used as building blocks in the construction of the excitation spectrum. This procedure allows for a large simplification in the description of the states. Therefore, it is possible to understand this region of excitation (which otherwise appears to be too complicated in other microscopic representations) in terms of very simple degrees of freedom.

ACKNOWLEDGMENTS

Discussions with B. Bayman, A. Bohr, E. R. Flynn, G. Igo, B. Mottleson, and N. Stein are gratefully acknowledged.

APPENDIX I

We define the multipole pairing residual interaction as a separable force whose matrix elements have the same phase as the matrix elements of a δ force. This is a simple extension of the method used to define the usual (monopole) pairing force matrix elements (see, for instance, Ref. 10).

The matrix elements of a δ force in the singlet case (S state of relative motion) is equal to

$$\langle[\varphi_1(n_3 l_3 \tfrac{1}{2}; j_3)\varphi_2(n_4 l_4 \tfrac{1}{2}; j_4)]^\lambda_\mu | \delta(\vec{r}_1 - \vec{r}_2) | [\varphi_1(n_1 l_1 \tfrac{1}{2}; j_1)\varphi_2(n_2 l_2 \tfrac{1}{2}; j_2)]^\lambda_\mu \rangle$$
$$= N(n_1 l_1 j_1, n_2 l_2 j_2; \lambda\mu) N(n_3 l_3 j_3; n_4 l_4 j_4; \lambda\mu) F(n_1 l_1, n_2 l_2, n_3 l_3, n_4 l_4), \tag{A1.1}$$

where

$$\varphi_1(n l \tfrac{1}{2}; jm) = (-1)^{(N-1)/2} u_l(r)[Y_l(\theta_1, \varphi_1)\chi^{1/2}(\sigma_1)]^j_m, \tag{A1.2}$$

$$N(n_1 l_1 j_1, n_2 l_2 j_2; \lambda\mu) = (-1)^{(N_1 - l_1)/2}(-1)^{(N_2 - l_2)/2}(-1)^{l_1 + j_2 + \lambda + \frac{1}{2}} \left[\frac{(2j_1+1)(2j_2+1)}{2}\right]^{1/2}$$
$$\times \begin{Bmatrix} \lambda & j_1 & j_2 \\ \frac{1}{2} & l_2 & l_1 \end{Bmatrix} \left[\frac{(2l_1+1)(2l_2+1)}{4\pi(2\lambda+1)}\right]^{1/2} (l_1 l_2 00|\lambda 0), \tag{A1.3}$$

$$F(n_1 l_1, n_2 l_2, n_3 l_3, n_4 l_4) = \int u_{n_3 l_3}^*(r) u_{n_4 l_4}^*(r) u_{n_1 l_1}(r) u_{n_2 l_2}(r) r^2 dr. \tag{A1.4}$$

The Condon-Shortley phase convention is used for the spherical harmonics and the function $u_{nl}(r)$ is positive for large values of r. Then, $F(n_1l_1, n_2l_2, n_3l_3, n_4l_4)$ is positive for the most usual single-particle potentials used to calculate $u_{nl}(r)$. On the other hand the function $(-1)^{(N-l)/2}u_{nl}(r)$ is positive for $r \to 0$. This is the usual convention chosen in shell-model-type calculations.

It is known that an operator which does not contain spin coordinates has large matrix elements between states that do not change the spin orientation with respect to the orbital angular momentum. In particular, for the classical limit ($j \to \infty$) the weak component of the matrix element (i.e., those involving spin flip) vanish. In the present case, $N(n_1l_1j_1, n_2l_2j_2) = 0$ unless both single-particle states are of the type $j = l + \frac{1}{2}$ or $j = l - \frac{1}{2}$.

The limit of (A1.3) for j_1 and $j_2 \to \infty$ is equal to

$$\lim_{\substack{j_1 j_2 \to \infty \\ (\lambda \ll j_1, j_2)}} N(n_1l_1j_1, n_2l_2j_2; \lambda\mu) \approx (-1)^{l_1+j_2+\lambda+\frac{1}{2}}\left[\frac{(2j_2+1)(2j_1+1)}{2}\right]^{1/2} \times \begin{Bmatrix} \lambda & j_1 & j_2 \\ \frac{1}{2} & l_2 & l_1 \end{Bmatrix} (-1)^{(N_1-l_1)/2}(-1)^{(N_2-l_2)/2}[(-1)^{l_1+l_2+\lambda}+1]C_{\lambda, l_1-l_2}\left(\frac{2l_2+1}{2\lambda+1}\right)^{1/2}. \quad \text{(A1.5)}$$

The magnitude $C_{\lambda_1 j_1 - j_2}$ is a positive C number. Use has been made of the relation

$$\lim_{\substack{j_2 \to \infty \\ (\lambda \ll j_2)}} \langle j_2\tfrac{1}{2}\lambda 0 | j_1\tfrac{1}{2}\rangle \approx (-1)^{j_2+\lambda-j_1}(-1)^{\lambda-j_2+j_2}d_{j_1-j_2,0}(\tfrac{1}{2}\pi) = (-1)^{j_1-j_2}\left(\frac{4\pi}{2\lambda+1}\right)^{1/2} C_{\lambda, j_1-j_2}(-1)^{(j_1-j_2+\lambda)/2}[(-1)^{j_1-j_2+\lambda}+1]. \quad \text{(A1.6)}$$

With the aid of Eq. (6.3.4) of Edmunds,[28] we obtain

$$\lim_{\substack{j_1, j_2 \to \infty \\ (\lambda \ll j_1, j_2)}} (-1)^{l_1+j_2+\lambda+\frac{1}{2}}\left[\frac{(2j_2+1)(2j_1+1)}{2}\right]^{1/2}\begin{Bmatrix} \lambda & j_1 & j_2 \\ \frac{1}{2} & l_2 & l_1 \end{Bmatrix} = \frac{1}{\sqrt{2}} \quad \text{(A1.7)}$$

both for ($j_1 = l_1 + \frac{1}{2}$, $j_2 = l_2 + \frac{1}{2}$) and for ($j_1 = l_1 - \frac{1}{2}$, $j_2 = l_2 - \frac{1}{2}$). We can then write Eq. (A1.5) as

$$N(l_1j_1, l_2j_2; \lambda\mu) \approx \left[\frac{1}{\sqrt{2}}\left(\frac{2l_2+1}{2\lambda+1}\right)^{1/2} C_{\lambda_1 l_1 - l_2}\right][(-1)^{l_1+l_2+\lambda}+1](-1)^{(l_1+l_2+\lambda)/2}(-1)^{(N_1-l_1)/2}(-1)^{(N_2-l_2)/2}. \quad \text{(A1.8)}$$

The matrix element of the multipole pairing field is required to have the same phase as (A1.8). Thus the pairing force will have matrix elements with the same phase as the ones defined in Eq. (A1.1).

The reduced matrix element of $f_\lambda(r)Y_{\lambda\mu}$ is equal to

$$\langle \varphi(n_1l_1\tfrac{1}{2}; j_1) \| f_\lambda(r)Y_\lambda(\theta,\phi) \| \varphi(n_2l_2\tfrac{1}{2}; j_2)\rangle = (-1)^{l_1+l_2+j_1-j_2}\left[\frac{(2\lambda+1)(2j_2+1)}{4\pi}\right]^{1/2}(-1)^{(N_2-l_2)/2}(-1)^{(N_1-l_1)/2}\langle j_2\tfrac{1}{2}\lambda 0 | j_1\tfrac{1}{2}\rangle I(n_1l_1, n_2l_2, \lambda), \quad \text{(A1.9)}$$

where

$$I(n_1l_1, n_2l_2, \lambda) = \int u_{n_1l_1}{}^*(r) f_\lambda(r) u_{n_2l_2}(r) r^2 dr. \quad \text{(A1.10)}$$

The sign of $I(n_1l_1, n_2l_2, \lambda)$ depends on λ, but is independent of l_1 and l_2. In the classical limit Eq. (A1.9) is equal to

$$\lim_{\substack{j_1, j_2 \to \infty \\ (\lambda \ll j_1, j_2)}} \langle \varphi(n_1l_1\tfrac{1}{2}; j_1) \| f_\lambda(r)Y(\theta,\phi) \| \varphi(n_2l_2\tfrac{1}{2}; j_2)\rangle \approx \left[\left(\frac{2j_2+1}{4\pi}\right)^{1/2} C_{\lambda_1 l_1 - l_2} I(n_1l_1, n_2l_2, \lambda)\right](-1)^{l_1}[(-1)^{l_1+l_2+\lambda}+1](-1)^{(l_1+l_2+\lambda)/2}(-1)^{(N_1-l_1)/2}(-1)^{(N_2-l_2)/2}, \quad \text{(A1.11)}$$

where as in Eq. (A1.4) $j_i = l_i \pm \frac{1}{2}$ ($i = 1, 2, 3, 4$). By comparing Eqs. (A1.8) and (A1.11) we see that the pairing field must be defined as

$$P_{\lambda\mu}{}^\dagger = m(\lambda) \sum_{\substack{n_1l_1j_1 \\ n_2l_2j_2}} (-1)^l \langle \varphi(n_1l_1\tfrac{1}{2}; j_1) \| f_\lambda(r)Y_\lambda(\theta,\phi) \| \varphi(n_2l_2\tfrac{1}{2}; j_2)\rangle \frac{[a_{l_1j_1}{}^\dagger a_{l_2j_2}{}^\dagger]^\lambda_\mu}{(1+\delta_{12})^{1/2}}, \quad \text{(A1.12)}$$

where $a_{ljm}{}^\dagger$ creates a particle in an orbital (lj) and transforms under time reversal as $\tau a_{ljm}{}^\dagger \tau^{-1}$

$= (-1)^{j+j-m} a_{jj-m}{}^{\dagger}$ (Condon-Shortley phase convention). The magnitude $m(\lambda)$ is a c number that depends only on λ. We can recast Eq. (A1.12) in terms of the $b_{jj}{}^{\dagger}$ operators (for simplicity we have not included in the text l as an explicit label of the $b^{\dagger}$ operators) defined in Eq. (2d) of Sec. III A. The relation between the $a_{jj}{}^{\dagger}$ and $b_{jj}{}^{\dagger}$ operators is

$$b_{jj}{}^{\dagger} = i^{j} a_{jj}{}^{\dagger}. \tag{A1.13}$$

Making $m(\lambda) = -2i^{\lambda}/(2\lambda+1)^{1/2}$ we obtain

$$P_{\lambda\mu}{}^{\dagger} = -\frac{2}{(2\lambda+1)^{1/2}} \sum_{\substack{n_1 l_1 j_1 \\ n_2 l_2 j_2}} i^{l_2 - l_1 + \lambda} \langle \varphi(n_1 l_1 \tfrac{1}{2}; j_1) \| f_{\lambda}(r) Y_{\lambda}(\theta,\phi) \| \varphi(n_2 l_2 \tfrac{1}{2}; j_2) \rangle \frac{[b_{l_1 j_1}{}^{\dagger} b_{l_2 j_2}{}^{\dagger}]^{\lambda}_{\mu}}{(1+\delta_{12})^{1/2}} \tag{A1.14}$$

which is given in Eq. (2a). We should point out that, although we have imposed phase requirements only on the strong components of the matrix elements of the operator (A1.14), the weak components of these matrix elements (i.e., the components implying spin flip) have the same phase as the corresponding components of the matrix elements of the δ force.

We turn now our attention to the multipole particle-hole operator defined in Eq. (10) of Sec. II. Adopting the Condon-Shortley phase convention the n-pole operator is customarily written as

$$\begin{aligned} Q_{\lambda\mu} &= \sum_{\substack{n_1 l_1 j_1 m_1 \\ n_2 l_2 j_2 m_2}} \langle \varphi(n_1 l_1 \tfrac{1}{2}; j_1 m_1 | r^{\lambda} Y_{\lambda\mu}(\theta\phi) | \varphi(n_2 l_2 \tfrac{1}{2}; j_2 m_2) \rangle a_{l_1 j_1 m_1}{}^{\dagger} a_{l_2 j_2 m_2} \\ &= \frac{1}{(2\lambda+1)^{1/2}} \sum_{\substack{n_1 l_1 j_1 \\ n_2 l_2 j_2}} \langle \varphi(n_1 l_1 \tfrac{1}{2}; j_1) \| r^{\lambda} Y_{\lambda}(\theta,\phi) \| \varphi(n_2 l_2 \tfrac{1}{2}; j_2) \rangle [a_{l_1 j_1}{}^{\dagger} a_{l_2 j_2}]^{\lambda}_{\mu}, \end{aligned} \tag{A1.15}$$

where the definition (13a) of Sec. II B for the vector coupling square brackets has been used. We can rewrite Eq. (A1.15) in terms of the $b_{jj}{}^{\dagger}$ operators. To obtain real matrix elements we should use the operator $i^{\lambda} r^{\lambda} Y_{\lambda}$ instead of $r^{\lambda} Y_{\lambda}$. We finally obtain

$$Q_{\lambda\mu} = -\frac{1}{(2\lambda+1)^{1/2}} \sum_{\substack{n_1 l_1 j_1 \\ n_2 l_2 j_2}} i^{l_2 - l_1 + \lambda} \langle \varphi(n_1 l_1 \tfrac{1}{2}; j_1) \| r^{\lambda} Y_{\lambda}(\theta,\phi) \| \varphi(n_2 l_2 \tfrac{1}{2}; j_2) \rangle [b_{l_1 j_1}{}^{\dagger} b_{l_2 j_2}]^{\lambda}_{\mu} \tag{A1.16}$$

which is identical to Eq. (10).

APPENDIX II

We denote by $|jm\rangle$ the single-particle states $b_{km}{}^{\dagger}|0\rangle$ (if $j=k$) or the single-hole states $(-1)^{i-m} b_{i-m}|0\rangle$ (if $j=i$). Similarly, the ket $|j_1 j_2, \lambda_{\mu}\rangle$ corresponds to the $[b_k{}^{\dagger} b_i]^{\lambda}_{\mu}|0\rangle$, the $[b_{k_1}{}^{\dagger} b_{k_2}{}^{\dagger}]^{\lambda}_{\mu}|0\rangle$, or the $[b_i\, b_i\,]^{\lambda}_{\mu}|0\rangle$ states, according to the position of the single-particle levels j_1, j_2. In addition, $|n\alpha\lambda\mu\rangle = \beta_n(\alpha\lambda\mu)|0\rangle$. With this notation plus the one given in Eq. (23), the matrix elements corresponding to Figs. 2 and 3 are

$$\langle n0\lambda\mu | h(0\lambda) | ki, \lambda \rangle = -\Lambda_n(0\lambda) M(ki;\lambda) \qquad [\text{Fig. 1(a)}], \tag{A2.1}$$

$$\langle 0 | h(0\lambda) | n0\lambda; ki\,; 00 \rangle = -(2\lambda+1)^{1/2} \Lambda_n(0\lambda) M(ki;\lambda) \qquad [\text{Fig. 1(b)}], \tag{A2.2}$$

$$\langle i_1 m | h(0\lambda) | n0\lambda; i_2; i_1 m \rangle = -\left(\frac{2\lambda+1}{2i_1+1}\right)^{1/2} \Lambda_n(0\lambda) M(i_1 i_2;\lambda) \qquad [\text{Fig. 1(c)}], \tag{A2.3}$$

$$\langle k_1 m | h(0\lambda) | n0\lambda; k_2; k_1 m \rangle = \left(\frac{2\lambda+1}{2k_1+1}\right)^{1/2} \Lambda_n(0\lambda) M(k_1 k_2;\lambda) \qquad [\text{Fig. 1(d)}], \tag{A2.4}$$

$$\langle n2\lambda\mu | h(+2\lambda) | k_1 k;\lambda \rangle = -\Lambda_n(2\lambda) M(k_1 k_2, \lambda) \qquad [\text{Fig. 2(a)}], \tag{A2.5}$$

$$\langle km | h(2\lambda) | n2\lambda; i; km \rangle = -\left(\frac{2\lambda+1}{2k+1}\right)^{1/2} \Lambda_n(2\lambda) M(ik, \lambda) \qquad [\text{Fig. 2(b)}], \tag{A2.6}$$

$$\langle 0 | h(2\lambda) | n2\lambda; i_1 i_2 \lambda; 00 \rangle = (2\lambda+1)^{1/2} \Lambda_n(2\lambda) M(k_1 k_2;\lambda) \qquad [\text{Fig. 2(c)}], \tag{A2.7}$$

$$\langle n -2\lambda\mu | h(2\lambda) | i_1 i_2, \lambda \rangle = \Lambda_n(-2\lambda) M(i_1 i_2;\lambda) \qquad [\text{Fig. 2(d)}], \tag{A2.8}$$

$$\langle i|h(+2\lambda)|n-2\lambda;k;im\rangle = -\left(\frac{2\lambda+1}{2i+1}\right)^{1/2}\Lambda_n(-2\lambda)M(ki;\lambda) \qquad \text{[Fig. 2(e)]}, \tag{A2.9}$$

$$\langle 0|h(+2\lambda)|n-2\lambda;k_1k_2\lambda;00\rangle = -(2\lambda+1)^{1/2}\Lambda_n(-2\lambda)M(k_1k_2;\lambda) \qquad \text{[Fig. 2(f)]}. \tag{A2.10}$$

APPENDIX III

The matrix elements of the effective Hamiltonian are given here. The energy denominators ΔE are to be constructed using either one of the prescriptions discussed in Sec. IV B.

$$\langle n_2 0\lambda_2;k_2;IM|H_{\text{eff}}|n_1 0\lambda_1;k_1;IM\rangle$$

$$= \Lambda_{n_1}(0\lambda_1)\Lambda_{n_2}(0\lambda)\frac{(2\lambda_1+1)^{1/2}(2\lambda_2+1)^{1/2}}{2I+1}\sum_j \delta_{jI}s_j M(k_2j;\lambda_2)M(k_1j;\lambda_1)/\Delta E \qquad \text{[Figs. 6 (e), 6(h)]}, \tag{A3.1}$$

$$\langle n_2 2\lambda_2;i_2;IM|H_{\text{eff}}|n_1 2\lambda_1;k_1;IM\rangle$$

$$= \Lambda_{n_1}(2\lambda_1)\Lambda_{n_2}(2\lambda_2)(2\lambda_1+1)^{1/2}(2\lambda_2+\ )^{1/2}\sum_j \delta_{jI}s_j M(i_2j;\lambda_2)M(i_1j;\lambda_1)/\Delta E \qquad \text{[Figs. 6(i), 6(j)]}, \tag{A3.2}$$

$$\langle n_2 0\lambda_2;k_2;IM|H_{\text{eff}}|n_1 2\lambda_1;i_1;IM\rangle$$

$$= -\Lambda_{n_1}(2\lambda_1)\Lambda_{n_2}(0\lambda_2)\frac{(2\lambda_1+1)^{1/2}(2\lambda_2+1)^{1/2}}{2I+1}\sum_j \delta_{ji}s_j M(k_2j;\lambda_2)M(i_1j;\lambda_1)/\Delta E \qquad \text{[Figs. 6(e), 6(d)]}, \tag{A3.3}$$

$$\langle n_2 0\lambda_2;k_2;IM|H_{\text{eff}}|n_1 0\lambda_1;i_1;IM\rangle$$

$$= -\Lambda_{n_1}(0\lambda_1)\Lambda_{n_2}(0\lambda_2)(2\lambda_1+1)^{1/2}(2\lambda_2+1)^{1/2}\sum_j s_j \begin{Bmatrix} j & k_2 & \lambda_1 \\ I & k_1 & \lambda_2 \end{Bmatrix} M(k_2j;\lambda_1)M(k_1j;\lambda_2)/\Delta E \qquad \text{[Figs. 6(e), 6(f)]}, \tag{A3.4}$$

$$\langle n_2 0\lambda_2;k_2;IM|H_{\text{eff}}|n_1 2\lambda;i_1;IM\rangle$$

$$= \Lambda_{n_1}(2\lambda_1)\Lambda_{n_2}(0\lambda_2)(2\lambda_1+1)^{1/2}(2\lambda j+1)^{1/2}\sum_j s_j \begin{Bmatrix} j & k_2 & \lambda_1 \\ I & i_1 & \lambda_2 \end{Bmatrix} M(k_2j;\lambda_1)M(i_1j;\lambda_2)/\Delta E \qquad \text{[Figs. 6(a), 6(b)]}, \tag{A3.5}$$

where

$$s_j = 1 \quad (\text{if } j=k)$$
$$= -1 \quad (\text{if } j=i).$$

APPENDIX IV

In this appendix we give the matrix elements corresponding to the second-order effective operator B_1 for the pickup reactions. Equations (A4.1)–(A4.4) correspond to the graphs of Fig. 7 and Eqs. (A4.5)–(A4.8) to the graphs of Figs. 8 and 9. The first cases represent the fact that a single-hole in ^{207}Pb may be scattered into a two-hole, one-particle state, and therefore the amount of time during which the pickup process can take place is effectively shortened.

$$\langle 120;i_2;i_2m|B_{i_2}\beta_1{}^{\dagger}(200)|0\rangle$$

$$= -\frac{1}{2}\frac{1}{(2i_2+1)}\sum_{\lambda,n}(2\lambda+1)\Lambda_n{}^2(-2\lambda)\sum_k \frac{M(ki_2;\lambda)^2}{[\epsilon_k+\epsilon_{i_2}-2\epsilon_{p_{1/2}}-\Delta W_n(-2\lambda)]^2} \qquad \text{[Fig. 7(b)]}, \tag{A4.1}$$

$$\langle 120;i_2;i_2m|B_i\ \beta_1{}^{\dagger}(200)|0\rangle$$

$$= -\frac{1}{2}\frac{1}{(2i_2+1)}\sum_{\lambda,n}(2\lambda+1)\Lambda_n{}^2(2\lambda)\sum_i \frac{M(ii_2;\lambda)^2}{[2\epsilon_{g_{9/2}}-\epsilon_i-\epsilon_{i_2}-\Delta W_n(2\lambda)]^2} \qquad \text{[Figs. 7(c), 7(d)]}, \tag{A4.2}$$

$$\langle 120;i_2;i_2m|B_{i_2}\beta_1{}^{\dagger}(200)|0\rangle$$

$$= -\frac{1}{2}\frac{1}{(2i_2+1)}\sum_{\lambda,n}(2\lambda+1)\Lambda_n{}^2(0\lambda)\sum_i \frac{M(ii_2;\lambda)^2}{[\epsilon_{g_{9/2}}+\epsilon_{i_2}-\epsilon_{p_{1/2}}-\epsilon_i-\Delta W_n(0\lambda)]^2} \qquad \text{[Fig. 7(i)]}, \tag{A4.3}$$

$$\langle 120; i_2; i_2 m|B_{i_2}\beta_1{}^{\dagger}(200)|0\rangle$$

$$= -\frac{1}{2}\frac{1}{(2i_2+1)}\sum_{\lambda,n}(2\lambda+1)\Lambda_n{}^2(0\lambda)\sum_k \frac{M(ki_2;\lambda)^2}{[\epsilon_{g_{9/2}}+\epsilon_k-\epsilon_{p_{1/2}}-\epsilon_{i_2}-\Delta W_n(0\lambda)]^2} \quad \text{[Figs. 7(f), 7(g)]}, \quad \text{(A4.4)}$$

$$\langle n2\lambda; im|B_i\beta_1{}^{\dagger}(200)|0\rangle$$

$$= \Lambda_1(20)\Lambda_n(2\lambda)\left(\frac{2\lambda+1}{2i+1}\right)^{1/2}\frac{M(i_2 i;\lambda)}{2\epsilon_{g_{9/2}}-\epsilon_{p_{1/2}}-\epsilon_i-\Delta W_n(2\lambda)}\frac{M(ii;0)}{2\epsilon_{g_{9/2}}-2\epsilon_i-\Delta W_1(20)} \quad \text{[Fig. 8(f)]}, \quad \text{(A4.5)}$$

$$\langle n0\lambda; k_2; im|B_i\beta_1{}^{\dagger}(200)|0\rangle$$

$$= -\Lambda_1(20)\Lambda_n(0\lambda)\left(\frac{2\lambda+1}{2i+1}\right)^{1/2}\left[\frac{M(k_2 i;\lambda)}{\epsilon_{g_{9/2}}+\epsilon_{k_2}-\epsilon_{p_{1/2}}-\epsilon_i-\Delta W_n(0\lambda)}\frac{M(ii;0)}{2\epsilon_{g_{9/2}}-2\epsilon_i-\Delta W_1(20)}\right.$$

$$\left.+\sum_{k_2}\frac{1}{(2k_2+1)^{1/2}}\frac{M(k_2 i;\lambda)}{\epsilon_{k_2}-\epsilon_{g_{9/2}}+\epsilon_{p_{1/2}}-\epsilon_i+\Delta W_n(0\lambda)}\frac{M(k_2 k_2;0)}{2(\epsilon_{k_2}-\epsilon_{g_{9/2}})+\Delta W(20)}\right] \quad \text{[Figs. 8(g), 8(h)]}, \quad \text{(A4.6)}$$

$$\langle n2\lambda; i_2; km|B_k\beta_1{}^{\dagger}(200)|0\rangle$$

$$= \Lambda_1(20)\Lambda_n(2\lambda)\left(\frac{2\lambda+1}{2k+1}\right)^{1/2}\frac{M(i_2 k;\lambda)M(kk;0)}{2(\epsilon_k-\epsilon_{g_{9/2}})+\Delta W_1(20)}\left[\frac{1}{\epsilon_k-\epsilon_{i_2}+\Delta W_1(20)-\Delta W_n(2\lambda)}\right.$$

$$\left.+\frac{1}{\epsilon_k-2\epsilon_{g_{9/2}}+\epsilon_{i_2}+\Delta W_n(2\lambda)}\right] \quad \text{[Figs. 9(a), 9(b)]}, \quad \text{(A4.7)}$$

$$\langle n0\lambda; k_2; km|B_k\beta_1{}^{\dagger}(200)|0\rangle$$

$$= -\Lambda_1(20)\Lambda_n(0\lambda)\left(\frac{2\lambda+1}{2k+1}\right)^{1/2}\left\{\frac{M(k_2 k;\lambda)M(kk0)}{2(\epsilon_k-\epsilon_{g_{9/2}})+\Delta W_1(20)}\right.$$

$$\times\left[\frac{1}{\epsilon_k+\epsilon_{p_{1/2}}-\epsilon_{k_2}-\epsilon_{g_{9/2}}+\Delta W_n(0\lambda_2)}+\frac{1}{\epsilon_{k_2}+\epsilon_k-\epsilon_{g_{9/2}}-\epsilon_{p_{1/2}}+\Delta W_1(20)-\Delta W_n(0\lambda)}\right]$$

$$\left.-\frac{1}{(2k+1)^{1/2}}\frac{M(k_2 k;\lambda)}{\epsilon_{k_2}+\epsilon_k-\epsilon_{g_{9/2}}-\epsilon_{p_{1/2}}-\Delta W_n(0\lambda)}\frac{M(k_2 k_2;0)}{2\epsilon_{k_2}-2\epsilon_{g_{9/2}}+\Delta W_1(20)}\right\} \quad \text{[Figs. 9(c)–9(e)]}.$$

(A4.8)

APPENDIX V

Appendix V includes the matrix elements corresponding to the two-body transfer reaction (see Fig. 10).

$$\langle n2\lambda_2; i_2; IM|[T_\lambda^{(\nu)}(k,k')b_{p_{1/2}}]_M^I|0\rangle$$

$$= \delta_{\lambda_1\lambda_2}\delta_{i_2 p_{1/2}}\Lambda_n(2\lambda_2)\frac{M(kk';\lambda)}{\epsilon_{k'}+\epsilon_k-2\epsilon_{g_{9/2}}+\Delta W_n(2\lambda_2)} \quad \text{[Fig. 11(a)]}, \quad \text{(A5.1)}$$

$$\langle n2\lambda_2; i_2; IM|[T_\lambda^{(\nu)}(i,i')b_{p_{1/2}}]_M^I|0\rangle$$

$$= \delta_{\lambda_1\lambda_2}\delta_{i_2, p_{1/2}}\Lambda_n(2\lambda_2)\frac{M(ii';\lambda)}{2\epsilon_{g_{9/2}}-\epsilon_i-\epsilon_{i'}-\Delta W_n(2\lambda_2)} \quad \text{[Fig. 11(b)]}, \quad \text{(A5.2)}$$

$$\langle n2\lambda_2; i_2; IM|[T_\lambda^{(\nu)}(j,p_{1/2})b_{p_{1/2}}]_M^I|0\rangle$$

$$= -\delta_{jI}\Lambda_n(2\lambda_2)\frac{(2\lambda_2+1)^{1/2}(2\lambda+1)^{1/2}}{2I+1}\frac{M(i_2 j;\lambda_2)}{\epsilon_j+\epsilon_{i_2}-2\epsilon_{g_{9/2}}+\Delta W_n(2\lambda_2)} \quad \text{[Figs. 11(c), 11(d)]}, \quad \text{(A5.3)}$$

$$\langle n0\lambda_2; k_2; IM|[T_\lambda^{(1)}(k_2;j)b_{p_{1/2}}]_M^I|0\rangle$$
$$= -\Lambda_n(0\lambda_2)(-1)^{\lambda_2+j+\frac{1}{2}}(2\lambda_2+1)^{1/2}(2\lambda+1)^{1/2}\begin{Bmatrix} k_2 & j & \lambda \\ \frac{1}{2} & I & \lambda_2 \end{Bmatrix}\frac{M(jp_{1/2};\lambda_2)}{\epsilon_j-\epsilon_{g_{9/2}}+\Delta W_n(0\lambda_2)} \quad \text{[Figs. 11(e), 11(f)]}, \quad \text{(A5.4)}$$

$$\langle n0\lambda_2; k_2; IM|[T_\lambda^{(1)}(j,p_{1/2})b_{p_{1/2}}]_M^I|0\rangle$$
$$= -\Lambda_n(0\lambda_2)\delta_{jI}(-1)^{1/2+\lambda+I}\frac{(2\lambda_2+1)^{1/2}(2\lambda+1)^{1/2}}{(2I+1)}\frac{M(k_2j;\lambda_2)}{\epsilon_{k_2}+\epsilon_{g_{9/2}}-\epsilon_j-\epsilon_{p_{9/2}}-\Delta W_n(0\lambda_2)} \quad \text{[Figs. 11(g), 11(h)]}. \quad \text{(A5.5)}$$

*Work performed under the auspices of the U. S. Atomic Energy Commission, Contract No. AT(11-1)1764 and W-7405-ENG-36.

†Present address: Niels Bohr Institute, University of Copenhagen, Copenhagen, Denmark.

[1]A. Bohr, Compt. Rend. Congr. Intern. Phys. Nucl., Paris, 1964, 1, 487 (1964).

[2]For instance, A. Kerman, Kgl. Danske Videnskab. Selskab., Mat.-Fys. Medd. 30, No. 15 (1956); M. I. Cherney, N. I. Pyatov, in *Proceedings of the International Conference on Properties of Nuclear States, Montréal, Canada, 1969*, edited by M. Harvey *et al.* (Presses de l'Université de Montréal, Montréal, Canada, 1969), p. 1.

[3]For instance, D. C. Chondhury, Kgl. Danske Videnskab. Selskab, Mat.-Fys. Medd. 28, No. 4 (1954); L. S. Kisslinger and R. A. Sorensen, Rev. Mod. Phys. 35, 853 (1963); A. I. Sherwood and A. Goswami, Nucl. Phys. 89, 465 (1966); A91, 64 (1967); D. R. Bes and G. G. Dussel, *ibid.* A135, 1, 25 (1969).

[4]For instance, V. G. Soloviev and P. Vogel, Nucl. Phys. A92, 449 (1967); D. R. Bes and C. Yi-Chung, *ibid.* 86, 581 (1966).

[5]J. C. Hafele and R. Woods, Phys. Letters 20, 674 (1966); G. Igo, P. Barnes, E. R. Flynn, and R. Woods, J. Phys. Soc. Japan, Suppl. 24, 87 (1968); C. E. Ellegaard, J. Kantele, and P. Vedelsby, Phys. Letters 25B, 512 (1967); C. Ellegaard and P. Vedelsby, *ibid.* 26B, 155 (1967).

[6]B. R. Mottelson, J. Phys. Soc. Japan, Suppl. 24, 87 (1968).

[7]For example, I. Hamamoto, Nucl. Phys. A126, 545 (1969); A135, 576 (1969); A141, 1 (1970); R. A. Broglia, J. Damgaard, and A. Molinari, *ibid.* A127, 437 (1969); N. Auerbach and N. Stein, Phys. Letters 28B, 628 (1969); R. A. Broglia, J. Lilley, R. J. Perazzo, and R. Phillips, Phys. Rev. C 1, 1508 (1970).

[8]E. R. Flynn, G. Igo, P. D. Barnes, D. Kovar, D. Bes, and R. Broglia, following paper [Phys. Rev. C 3, 2371 (1971)]; E. R. Flynn, G. Igo, P. Barnes, and D. Kovar, Phys. Rev. Letters 22, 142 (1969); G. Igo, P. Barnes, E. Flynn, and B. Dropesky, Phys. Rev. C 3, 349 (1971).

[9]D. R. Bes and R. Broglia, Nucl. Phys. 80, 289 (1966); A. Bohr, in *Proceedings of the International Symposium on Nuclear Structure, Dubna, 1968* (International Atomic Energy Agency, Vienna, Austria, 1969), p. 169; O. Nathan, in *ibid.*, p. 191; D. R. Bes, R. A. Broglia, R. J. Perazzo, and K. Kumar, Nucl. Phys. A143, 1 (1970).

[10]D. R. Bes and R. Sorensen, *Advances in Nuclear Physics* (Plenum Press, Inc., New York, 1969), Vol. 2, p. 129; B. Bayman, "Seniority Quasiparticles, and Collective Vibrations," lectures given in the Palmer Physical Laboratory, Princeton University, 1960 (unpublished).

[11]Throughout this paper we use single-particle states obeying the symmetry relation [Eq. (2d)]. To obtain the Condon-Shortly phase required by most two-body transfer computer codes one should multiply the amplitudes given in this paper by i^L, where $L = l_{j_1} + l_{j_2} - \lambda$.

[12]This prescription can be used also in cases in which no absolute experimental cross sections are available. In this case, R is interpreted as a scaling factor. For a detailed discussion of the above-mentioned points in the text, see B. F. Bayman, Phys. Rev. Letters 25, 1768 (1971); to be published; and R. A. Broglia, C. Riedel, and T. Udagawa, to be published.

[13]Because of the requirement $\beta_n(\alpha\lambda\mu)|^{208}\text{Pb(g.s.)}\rangle = \beta_n(\alpha\lambda\mu)|0\rangle = 0$, the state $|0\rangle$ displays 2p-1h type of correlations. These correlations enhance the two-body transfer cross section to the $\beta_1^\dagger(\alpha\lambda\mu)|0\rangle$ states, through the constructive coherence of backward-going amplitudes.

[14]G. Igo, P. Barnes, and E. Flynn, Phys. Rev. Letters 24, 470 (1970).

[15]G. E. Brown and M. Bolsterli, Phys. Rev. Letters 3, 472 (1959); V. Gillet, A. M. Green, and E. A. Sanderson, Nucl. Phys. 88, 321 (1966); C. J. Veje, Kgl. Danske Videnskab. Selskab, Mat.-Fys. Medd. 35, No. 1 (1966).

[18]Use has been made of the relation

$$[b_k^\dagger b_i]_\mu^\lambda = \sum_n d_n(ki;0\lambda)\beta_n^\dagger(0\lambda\mu) + (-1)^{\lambda-\mu}\sum_n d_n(ik;0\lambda)\beta_n(0\lambda-\mu),$$

and of the one-phonon state wave function

$$\beta_n^\dagger(0\lambda\mu)|0\rangle = |(10\lambda)JM\rangle(\lambda=J),$$

where $|0\rangle$ is the N_0 system correlated ground state (see Sec. IV A).

[17]G. Bertsch, R. A. Broglia, and C. Riedel, Nucl. Phys. A91, 123 (1967); R. A. Broglia, C. Riedel, and T. Udagawa, to be published.

[18]D. R. Bes, G. G. Dussel, and J. Gratton, in *Proceedings of the International Conference on Nuclear Physics, Gatlinburg, Tennessee, 12–17 September 1966*, edited by R. L. Becker and A. Zucker (Academic Press Inc., New York, 1967), p. 499.

[19]The magnitude $(Q_{\lambda\mu})_{\text{coll}}$ takes the place of $\alpha_{\lambda\mu}$ variable in the standard formulation of the particle-vibration coupling Hamiltonian, whether $Q_{\lambda\mu}$ replaces $Y_{\lambda\mu}$.

[20]D. R. Bes and R. A. Broglia, Phys. Rev. C 3, 2349 (1971).

[21]This method was suggested to us by B. R. Mottelson.

[22]E. R. Flynn, G. Igo, P. Barnes, and D. Kovar, Phys.

Rev. Letters 22, 142 (1969).

[23]Because the single-hole states have different spin or parity than the single-particle states, and the ground state of ^{210}Pb has $\lambda = 0$, $\pi = +$, some graphs of Figs. 8 and 9 do not contribute because of general selection rules, namely 8, 9(a), and 9(b). The matrix elements corresponding to these cases are not given in Appendix IV.

[24]D. J. Thouless, *The Quantum Mechanics of Many-Body Systems* (Academic Press, New York, 1961).

[25]M. Redlich, Phys. Rev. 138, 544 (1964).

[26]C. T. Chen and F. W. Hurley, Nucl. Data B1, (No. 13), 1 (1966).

[27]We are indebted to Professor B. R. Mottelson for pointing out to us that a deficiency of the model is that our coupling Hamiltonian does not include some large matrix elements corresponding to the usual quadrupole particle-hole force.

[28]A. R. Edmonds, *Angular Momentum in Quantum Mechanics* (Princeton University Press, Princeton, New Jersey, 1967).